

TOPICAL REVIEW

# Neutrino flavour transformation in supernovae

H Duan<sup>1</sup> and J P Kneller<sup>2,3</sup>

<sup>1</sup> Institute for Nuclear Theory, University of Washington, Seattle, WA 98195, USA

<sup>2</sup> School of Physics and Astronomy, University of Minnesota, Minneapolis, MN 55455, USA

<sup>3</sup> Institut de Physique Nucléaire, F-91406 Orsay cedex, CNRS/IN2P3 and University of Paris-XI, France

E-mail: [huaiyu.duan@mailaps.org](mailto:huaiyu.duan@mailaps.org), [kneller@ipno.in2p3.fr](mailto:kneller@ipno.in2p3.fr)

**Abstract.** Rapid progress has been made during recent years in the understanding of the flavour oscillations that occur as neutrinos traverse through supernova. The previous paradigm has given way and it is now clear that the neutrino signals we shall receive from future Galactic supernovae will allow us both to peer inside these extraordinary cosmic events and to probe some of the fundamental properties of these elusive particles. In this review we aim to distill the progress that has been made focusing upon the effects of the dynamic density profile and the emergence of collective flavour oscillations due to neutrino self-interactions.

PACS numbers: 14.60.Pq, 97.60.Bw

## 1. Introduction

The detection of neutrinos from the Sun (Davis *et al.*, 1984, 1968) and Supernova 1987A (Alekseev *et al.*, 1987; Bionta *et al.*, 1987; Hirata *et al.*, 1987) have laid the foundation for a new field, neutrino astronomy. These discoveries not only opened a new window upon the Universe through the observation of cosmic neutrinos but also established a new way to probe fundamental properties of these elusive particles in the grand “laboratories” of stars or even the entire Universe. One such experiment was the Sudbury Neutrino Observatory (SNO) (Ahmad *et al.*, 2002) which showed that neutrinos other than  $\nu_e$ , the only neutrino species produced in the Sun, were present in the solar neutrino flux at Earth. This transformation to other flavours and the concomitant deficit in  $\nu_e$  — the solar neutrino problem (Bahcall and Sears, 1972) — can be elegantly explained by the Mikheyev-Smirnov-Wolfenstein (MSW) mechanism (Mikheyev and Smirnov, 1985; Wolfenstein, 1978). If neutrinos have masses and the flavour states are not the mass eigenstates, then the electron neutrinos emitted in the high density at the core of the Sun experience resonant flavour conversion as they propagate to the vacuum thereby altering the composition of the flux. SNO, other solar neutrino experiments, atmospheric neutrino experiments and also terrestrial experiments have now compiled compelling evidence that indeed neutrinos of different flavours can mutate into each other and this phenomenon is known as “neutrino flavour transformation” or “neutrino (flavour) oscillation” (see, e.g. Amsler *et al.*, 2008 for a review).

But the focus of this review is core-collapse supernova, which we will refer to simply as supernova from now on. The explosion marks the death of a star with mass greater than  $\sim 8M_\odot$  (see, e.g. Woosley *et al.*, 2002 for a review) initiated as the iron core of the star collapses when it is incapable of generating sufficient supporting thermal energy through further nuclear fusion (Weaver *et al.*, 1978). A proto neutron star (PNS) (Baade and Zwicky, 1934) forms at the centre of the supernova if the collapse can be halted after supra nuclear density is reached. Most of the gravitational binding energy ( $\sim 3 \times 10^{53}$  erg) of the PNS is released in the form of neutrinos of all species with energies  $\sim 10$  MeV over a period of 10 seconds or so. Supernovae are such luminous sources of neutrinos that a supernova located 10 kpc from Earth would flood a neutrino detector here with a flux of  $\sim 10^{11}$  cm<sup>-2</sup>s<sup>-1</sup>. Over the duration of the burst this flux is more or less the same as that from the Sun but with much larger average energy. With current neutrino detector technology we should observe at least several thousands from the next supernova in our Galaxy (Ahrens *et al.*, 2002; Beacom *et al.*, 2002; Cadonati *et al.*, 2002; Dornic *et al.*, 2008; Ikeda *et al.*, 2007; Sharp *et al.*, 2002).

Because supernova energetics are dominated by neutrinos, it was immediately realized after the discovery of the MSW mechanism that any neutrino flavour transformation in supernovae could have important effects (Fuller *et al.*, 1987). There are many flavour transformation scenarios that could occur in the supernovae but for this review we shall consider just the flavour transformation of active neutrinos outside the neutrino sphere where neutrinos start free streaming. In this regard the flavour transformation is similar to that in the Sun but there are three key aspects of neutrino flavour transformation in a supernova that also make it very different from the solar environment: (a) the matter density in a supernova is much higher ( $\rho \sim 10^{12}$  g cm<sup>-3</sup> at the neutrino sphere) so that oscillations can be affected by both neutrino mass-squared differences; (b) the density profile of a supernova is rich with

prominent features which evolve over the duration of the neutrino emission; and (c) the neutrino flux near the neutrino sphere can be so large that neutrino self-interaction must be taken into account. The vast majority of the neutrinos emitted by the PNS propagate through the overlying material unimpeded; only a small percentage will be absorbed by nucleons/nuclei. But due to neutrino oscillations what is detected here on Earth is not the same as that emitted by the PNS. The neutrino evolves as it propagates and for practical purposes the evolution to Earth is solved in a sequence of steps: first, we calculate the state at the surface of the supernova; second, we add on the effect of propagating through the vacuum to Earth; and third, an “Earth matter” effect (Dighe and Smirnov, 2000) is sometimes included to account for the possibility that the neutrinos may have to pass through the Earth before reaching a detector. Of the three steps in calculating the neutrino signal at Earth it is the first step, the calculation to the surface of the supernova, that is by far the most difficult and which forms the focus of this review. We should mention here that at the present time neutrino oscillations are not part of supernova simulations or are treated only approximately. So to date neutrinos are usually sent through the supernova in a post-processing stage, i.e. the supernova is an input.

### 1.1. MSW flavour transformation with dynamic density profiles

The first studies of the electron dominated/pure MSW effect in supernovae employed purely static density profiles. Temporal evolution of the profile was ignored and any time dependence of the neutrino signal was limited to the variation of the neutrino spectra emitted by the core. But in recent years this has changed and the density profiles used now have become increasingly sophisticated.

The first, generic, evolutionary feature of any core-collapse supernova is the forward shock. That a shock is formed in the supernova was discovered in the first simulations by Colgate and Johnson (1960) and the feature is generated by the rebound of the PNS during the implosion (Colgate *et al.*, 1961). Initially it was thought that the shock would then proceed to shed the mantle of the supernova, the so-called prompt explosion mechanism, but as the physics input into the simulations became more accurate it was eventually realised that actually the prompt explosion mechanism fails (Hillebrandt and Mueller, 1981; van Riper, 1982). The outward motion of the forward shock stalls at a distance  $\sim 200$  km from the PNS chiefly due to nuclear dissociation (Arnett, 1982; Mazurek, 1982). If the star is to explode the shock must be revived from its stalled position and this can only occur by heating the material behind the shock. Due to the prodigious amounts of energy they convey, the neutrinos streaming out from the PNS were invoked by Bethe and Wilson (1985) as the transporters of energy from the hot core to the region behind the shock. This current paradigm of a stalled shock that is later revived is termed the delayed explosion mechanism. Revival of a shock due to neutrino heating does appear to work in the limited case of stars in the mass range  $8\text{--}11 M_{\odot}$  which have O-Ne-Mg cores (Dessart *et al.*, 2006; Kitaura *et al.*, 2006). The explosion energies of the simulations are smaller than the typical observed energies of supernova by around an order of magnitude but such weak supernovae do seem to match the energetics of some faint,  $^{56}\text{Ni}$  deficient, Type II P supernovae (Chugai and Utrobin, 2000; Pastorello *et al.*, 2007). But for more massive stars where the core is composed of iron all spherically symmetric simulations of the supernova using Boltzmann neutrino transport do not explode (Hix *et al.*, 2003; Liebendörfer *et al.*, 2001; Mezzacappa *et al.*, 2001; Rampp and Janka, 2000; Thompson *et al.*, 2003).

Any simulation that does explode uses “gray” neutrino transport (Mezzacappa, 2005). While less satisfying than an explosion based upon first principles such simulations are, nonetheless, useful because we can learn from them which features we should expect to find when truly successful supernova simulations are performed. Schirato and Fuller (2002) — and later Lunardini and Smirnov (2003), Takahashi *et al* (2003), and Fogli *et al* (2003) — were the first to consider the effect of the dynamic profile upon the neutrinos. They demonstrated that the forward shock would race out through the mantle of the star and reach the H resonance region — a position we shall clarify in the next section — within the first couple of seconds. Upon arrival its presence in this region alters the adiabaticity of the neutrinos as they propagate through the supernova and thus the flavour content of the neutrino signal at Earth. This discovery that the evolution of the density profile alters the flavour composition of the neutrino signal is the reason that one now needs to use time dependent density profiles in order to make accurate predictions.

After Schirato and Fuller (2002) additional features in the profile were also found to influence the neutrinos. The energy deposition does not switch off once the forward shock is revived and has begun moving outwards again. The material close to the PNS continues to be heated and the effect is to create a wind with a velocity that increases with distance from the core (Duncan *et al*, 1986). This wind pushes against the slower moving material in front of it creating a bubble or cavity. If the post shock-revival energy deposition is even more vigorous the wind strength grows to the point where its velocity may supersede the local sound speed. This leads to the formation of a new shock in the profile that faces the PNS rather than the exterior (Burrows *et al*, 1995; Janka and Mueller, 1995), i.e. it is “reversed”. Compared to the forward shock, the reverse shock is much more skittish. The reverse shock can be so strong that it penetrates to densities below those in front of the forward shock and then later it can diminish in size as the wind abates and even stall and return to the core (Arcones *et al*, 2007; Kneller *et al*, 2008; Tomàs *et al*, 2004). The effect upon the neutrinos of the presence of the reverse shock in the the profile was first considered by Tomàs *et al* (2004). Unfortunately these authors unintentionally omitted the consequences of the correlation of the wavefunction between the multiple H resonances now present in the profile which can lead to phase effects. That multiple resonances can lead to phase effects had been discussed many years prior by Kuo and Pantaleone (1989b) but it was only recently that Fogli *et al* (2003), re-examining the profiles of Schirato and Fuller (2002), discovered the phase effects in supernova neutrinos. Further examples showing their presence were presented by Kneller and McLaughlin (2006) and then phase effects were discussed extensively by Dasgupta and Dighe (2007).

But the failure of the best one-dimensional (1D), first-principles simulations indicates that supernova must be a multi-dimensional phenomena requiring rotation, convection, magnetic fields and/or other multi-dimensional physics. If that is the case then one would expect any explosion to be aspherical with a density profile that varies with the line of sight. Observational evidence that supernova are aspherical has abounded for years: asphericity has been observed or is implied from observations of Supernova 1987A (Dotani *et al*, 1987; Erickson *et al*, 1988; Li *et al*, 1993; Matz *et al*, 1988; Sunyaev *et al*, 1987), from the Vela SNR (Aschenbach *et al*, 1995), from Cassiopeia A (Hughes *et al*, 2000; Hwang *et al*, 2004) and from many other supernova remnants (e.g. Katsuda *et al*, 2008; Leonard *et al*, 2006; Wang *et al*, 2001). And of course pulsars have been observed with astounding velocities with some approaching  $\sim 1500 \text{ km s}^{-1}$  (Chatterjee *et al*, 2005; Cordes *et al*, 1993; Lyne

and Lorimer, 1994; Taylor *et al.*, 1993; Winkler and Petre, 2007). As with the 1D simulations, all two-dimensional (2D) simulations studied so far with the state-of-the-art neutrino transport (Buras *et al.*, 2003, 2006; Mezzacappa *et al.*, 1998) have yet to explode. In their place, 2D gray codes have been used to study how asphericity could be generated. Initially the focus was upon neutrino driven convection but the anisotropy was found to be small and the pulsar velocities were only of a few hundred  $\text{km s}^{-1}$  (Burrows *et al.*, 1995; Janka and Mueller, 1994, 1996). While not sufficient to explain the observations these studies did note that their simulations contained other departures from asphericity: for example, distortions of the stalled shock were observed by Burrows *et al.* (1995) who described the shock surface in their simulations as botryoidal, i.e. resembling a bunch of grapes. It was further study of these distortions of the stalled shock that have led to the discovery by Blondin *et al.* (2003) of a new mechanism for generating asphericity in supernova. Blondin *et al.* (2003) found that small aspherical perturbations of a stalled, spherical accretion shock could quickly grow and develop large dipole and, to a lesser extent quadrupole, modes. This standing accretion shock instability (SASI) will play an important part of future supernova simulations and may be a key ingredient in achieving explosions based upon first principles. From the multi-dimensional simulations we find that each radial slice through the supernova still possess the common features of forward/reverse shocks and a global hot bubble region identified from 1D but superimposed will be a mixture of features typical of asphericity such as additional/internal shocks, local bubbles, turbulence, sound waves, etc. Of these additional features in the profile the one that has generated most interest is the turbulence. The effects of turbulence in supernova profiles was first considered by Sawyer (1990, 1994) and Loreti *et al.* (1995) then later expanded upon by Fogli *et al.* (2006a). The correlation function of the density fluctuations is an important determinant and a typical first assumption was that the fluctuations were  $\delta$ -correlated. However, it was pointed out by Benatti and Floreanini (2005) that such a correlation is rather idealised and so recently authors such as Friedland and Gruzinov (2006) and Choubey *et al.* (2007) have switched to considering Kolmogorov turbulence instead. Whatever the exact spectrum used the general result of all these studies is that turbulence of sufficient strength can lead to flavour depolarisation.

In summary, over the period of just a few years the density profiles used to study supernova neutrino oscillations have progressed from simple, static parameterisations to profiles taken from aspherical supernova simulations that contain numerous features that affect the neutrinos. Later in this review we will examine in greater detail the dynamics of the pure MSW effect and how the use of improved density profiles has altered our expectations of the information in the neutrino signal.

### 1.2. Neutrino self-interaction and collective neutrino flavour transformation

The contribution from neutrino-neutrino forward scattering, or neutrino self-interaction, was noted by some of the first studies of neutrino flavour transformation in stellar collapse (Fuller *et al.*, 1992, 1987) and in the early Universe (Nötzold and Raffelt, 1988). Shortly after Pantaleone (1992) pointed out the existence of off-diagonal elements of the neutrino self-interaction potential in the flavour basis, and this observation was then incorporated into the general formalism for neutrino flavour evolution laid out by Sigl and Raffelt (1993). From these early studies it quickly became obvious that the inclusion of neutrino self-interactions poses a formidable

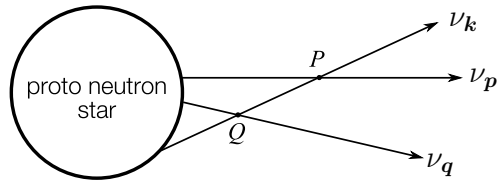


**Figure 1.** With neutrino self-interaction flavour evolution histories of neutrinos propagating along different but intersecting trajectories, e.g.  $\nu_k$  and  $\nu_q$ , are coupled because their flavour evolution histories beyond the intersection point,  $Q$ , will depend on the flavour states of both neutrinos at  $Q$ . In addition, the flavour evolution histories of non-intersecting neutrino beams such as  $\nu_p$  and  $\nu_q$  can also be coupled because the flavour evolution history of  $\nu_p$  beyond  $P$  indirectly depends on the flavour state of  $\nu_q$  at  $Q$  through  $\nu_k$ .

challenge (Qian and Fuller, 1995b). The reason for the complexity is illustrated in figure 1. The flavour evolution histories of any two neutrino beams becomes coupled due to the self-interaction and, as a result, in order to study the neutrino oscillations with neutrino self-interactions one needs to simultaneously follow the flavour evolution of all the neutrinos (with different energies, initial flavour states and propagating directions) emitted around the same time from all points on the neutrino sphere. We must emphasise that coupling of neutrino flavour evolution histories discussed in this review is, however, not quantum entanglement. The possible effects of the latter were discussed by, e.g. Bell *et al* (2003); Friedland and Lunardini (2003a,b).

Even for an idealised supernova model with a perfect spherical symmetry one must distinguish between the different neutrino trajectories along which neutrinos will have travelled different distances for the same radius interval. A simplifying approximation (but not necessarily a self-consistent treatment) was proposed by Qian and Fuller (1995b) who considered all the neutrino trajectories to be equivalent. In this “single-angle approximation” only the flavour evolution of neutrinos along one representative trajectory (e.g. the radially directed one) are computed.

In the two-flavour mixing scheme the flavour state of a neutrino can be represented as a classical spin or “magnetic dipole” in the three-dimensional flavour space (Kim *et al*, 1987; Mikheyev and Smirnov, 1986). Using this spin analogy Sigl and Raffelt (1993) showed that neutrino self-interaction is represented as coupling between these “flavour spins”. (We stress that a flavour spin is a fictitious spin in flavour space and that the spin analogy for neutrino oscillations discussed here is not related to flavour conversion of neutrinos because of coupling between the neutrino electromagnetic moment and a physical magnetic field considered by, e.g. Voloshin *et al* (1986).) While the early studies of neutrinos in supernova (Fuller *et al*, 1987; Qian and Fuller, 1995a,b; Qian *et al*, 1993) treated the self-interaction as an additional matter effect in the MSW mechanism, it is not inconceivable that the ensemble of flavour spins can exhibit collective behaviors in a similar fashion as spin gases in condensed matter physics. In fact, collective neutrino oscillation phenomena have been discussed in the context of the early Universe (e.g. Kostelecký and Samuel, 1995). One collective oscillation phenomenon which can appear in dense, homogeneous, isotropic neutrino gases is that, independent of their energy, all the neutrinos oscillate in the same way as a representative neutrino in vacuum (Samuel, 1993). This phenomenon is known as the synchronised neutrino oscillation because it can be explained in analogy to “a system of magnetic dipoles which are coupled by their self-interactions to

form one large magnetic dipole which then precesses coherently in a weak external magnetic field” (Pastor and Raffelt, 2002). Another collective oscillation phenomenon is known to occur in dense gases with approximately equal number of neutrinos and antineutrinos. Both neutrinos and antineutrinos can experience “substantial flavour oscillation even for extremely small mixing angles” if the neutrino mass hierarchy is inverted (Kostelecký and Samuel, 1993). This behaviour is usually known as the bipolar neutrino oscillation because it can be explained by using an analogy to a bipolar spin system which consists of two coupled and approximately oppositely-oriented groups of spins (Duan *et al*, 2006c).

Armed with this insight from neutrino behaviour in the early Universe and using the single-angle approximation Pastor and Raffelt (2002) and Balantekin and Yüksel (2005) showed that, in a normal neutrino mass hierarchy scenario, the combination of synchronisation and the MSW mechanism may indeed cause flavour conversion of both neutrinos and antineutrinos if the supernova neutrino luminosities are large enough. This phenomenon requires either a large mass-squared difference ( $\delta m^2 \simeq 10 \text{ eV}^2$ ) or a dilute supernova envelope so that the synchronised neutrinos encounter a MSW resonance near the neutrino sphere. Alternatively, Fuller and Qian (2006) envisioned a scenario where the off-diagonal part of the neutrino self-interaction potential dominates and both neutrinos and antineutrinos simultaneously achieve maximal mixing even for small mass-squared differences. This scenario is essentially a special case of synchronisation. Although Fuller and Qian (2006) identified necessary conditions for this scenario to occur, it is not clear if a realistic supernova event could evolve into this scenario even if these necessary conditions are satisfied. Then Duan *et al* (2006c) showed that a general bipolar neutrino system (e.g. with unequal numbers of neutrinos and antineutrinos) can exhibit collective flavour oscillations of either the synchronised or bipolar type if the total neutrino flux is larger or smaller than some critical value. In the same study Duan *et al* (2006c) also showed that ordinary matter has little effect on collective neutrino oscillations and that bipolar neutrino oscillations can occur very close to the neutrino sphere even if the matter density is large. Based on their analyses, Duan *et al* (2006c) mapped out the regimes in supernovae where synchronised, bipolar and conventional MSW neutrino oscillations may occur.

The first multi-angle (i.e. treating different neutrino trajectories as well as different neutrino energies) calculations of neutrino flavour transformation in supernovae were carried out by Duan *et al* (2006a,b). The results of their calculations show that, contrary to expectations based on the conventional MSW mechanism or synchronisation, both neutrinos and antineutrinos can simultaneously experience significant flavour oscillations near the neutrino sphere in some *inverted* neutrino mass hierarchy scenarios. Furthermore, when collective neutrino oscillations end, neutrinos of different flavours have their energy spectra swapped above a critical energy  $E_\nu^s$ , a phenomenon now known as “stepwise spectral swap” or “spectral split”. With density profiles and neutrino mixing parameters similar to those adopted by Balantekin and Yüksel (2005), Duan *et al* (2006a,b) observed similar spectral swap/split phenomenon with the normal mass hierarchy. They also carried out the single-angle calculations with setups similar to the multi-angle ones, and the results of single-angle and multi-angle calculations were found to bear many of the same qualitative features. This suggests that the single-angle approximation is a valid approach to study, at least qualitatively, neutrino oscillations in supernovae. Using the single-angle approximation Duan *et al* (2006b) also showed that the spectral swap/split phenomenon can be a result of collective neutrino oscillation mode in which

all flavour spins precess collectively. The discoveries made by [Duan \*et al\* \(2006a,b\)](#) have triggered intense and fruitful studies of collective neutrino oscillations in the supernova environment. Similar results were found in calculations using different neutrino mixing parameters and matter density profiles ([Duan \*et al\*, 2007b](#); [Fogli \*et al\*, 2007](#)) and even for some full three-flavour mixing scenarios ([Dasgupta and Dighe, 2008](#); [Duan \*et al\*, 2008b](#)). Signatures of these oscillation features in supernova neutrino signals have been investigated ([Chakraborty \*et al\*, 2008](#); [Dasgupta \*et al\*, 2008a](#); [Fogli \*et al\*, 2008](#); [Gava \*et al\*, 2009](#); [Lunardini \*et al\*, 2008](#)) and on the theoretical side collective neutrino oscillations in a single-angle approximated supernova model are now well understood ([Dasgupta and Dighe, 2008](#); [Dasgupta \*et al\*, 2008c](#); [Duan \*et al\*, 2007a,c, 2008d](#); [Hannestad \*et al\*, 2006](#); [Raffelt and Smirnov, 2007a,b](#)). Collective neutrino oscillations in anisotropic environments ([Duan \*et al\*, 2008c](#); [Esteban-Pretel \*et al\*, 2007](#); [Hannestad \*et al\*, 2006](#); [Raffelt and Sigl, 2007](#); [Sawyer, 2008](#)) and in non-spherical geometry ([Dasgupta \*et al\*, 2008b](#)) have also been examined. Effects of  $CP$ -violation ([Balantekin \*et al\*, 2008](#); [Gava and Volpe, 2008](#)) and the case of very large matter density ([Esteban-Pretel \*et al\*, 2008a,b](#)) have also been analysed. The recent progress in the understanding of neutrino self-interactions in supernovae has been impressive and, like the effect of the dynamic density profiles, has completely changed our expectations of the features in the neutrino signal we shall receive from the next Galactic supernova.

### 1.3. Organisation of the paper

Due to their importance in the explosion environment the neutrinos and their flavour transformation touch upon many different aspects of supernova phenomenology. For lack of space we cannot contemplate a comprehensive review of the entire field so we shall focus upon the specific topic of flavour transformation of active neutrinos as they propagate from the PNS to the supernova surface. In doing so we have left out many other interesting subjects such as neutrino nucleus interactions (e.g. [Balantekin and Fuller, 2003](#)), neutrino inelastic scattering (e.g. [Martínez-Pinedo, 2008](#)) and the possibility and consequences of sterile neutrinos (e.g. [Beun \*et al\*, 2006](#); [Fetter \*et al\*, 2003](#); [Fuller \*et al\*, 2009](#); [Hidaka and Fuller, 2007](#)). We will also not be able to address how one can begin to unpick the various signatures we now expect in an actual neutrino signal instead referring the reader to the literature (e.g. [Jachowicz and McLaughlin, 2006](#); [Jachowicz \*et al\*, 2008](#)). We begin with some general formalism of flavour transformation of supernova neutrinos in section 2. Historically the effects of dynamic matter density profiles and neutrino self-interaction have been studied in parallel, i.e. without inclusion of the effects caused by each other. So we will independently discuss the MSW flavour transformation with dynamic density profiles and collective flavour transformation in sections 3 and 4, respectively. Finally in section 5 we summarise and provide some outlook for where future advances lie.

## 2. Neutrino flavour transformation in supernovae: general discussions

### 2.1. Neutrino flavour transformation without neutrino self-interaction

Because neutrinos initially propagate coherently outside the neutrino sphere, the flavour state  $|\psi_{\mathbf{p}}(\mathbf{r})\rangle$  of a neutrino with momentum  $\mathbf{p}$  at point  $\mathbf{r}$  on its world line



can be solved from a Schrödinger-like equation (e.g. [Cardall, 2007](#); [Halprin, 1986](#))

$$i \frac{d}{d\lambda} |\psi_{\mathbf{p}}(\mathbf{r})\rangle = \hat{H}(\mathbf{r}) |\psi_{\mathbf{p}}(\mathbf{r})\rangle = [\hat{H}_{\text{vac}} + \hat{H}_{\text{matt}}(\mathbf{r}) + \hat{H}_{\nu\nu}(\mathbf{r})] |\psi_{\mathbf{p}}(\mathbf{r})\rangle, \quad (1)$$

where  $\lambda$  is the propagation distance of the neutrino along its world line,  $\hat{H}_{\text{vac}}$  is the Hamiltonian for vacuum oscillations,  $\hat{H}_{\text{matt}}(\mathbf{r})$  is from the forward scattering of the neutrino with the ordinary matter, and  $\hat{H}_{\nu\nu}(\mathbf{r})$  is the contribution from neutrino self-interaction. In equation (1) we have adopted the steady-state approximation. This is because neutrinos can traverse regions of interest within very short time, and the physical conditions in supernovae can barely change during this period. The flavour evolution of a neutrino along its world line can, therefore, be solved from a static configuration as outlined in equation (1). We first consider the scenarios that neutrino self-interaction can be ignored, i.e.  $\hat{H}_{\nu\nu}(\mathbf{r}) = 0$ .

There are two fundamental bases for the neutrinos: the flavour states  $|\nu_{\alpha}\rangle$  ( $\alpha = e, \mu, \tau$ ) which are the states seen in detectors, and the vacuum mass states  $|\nu_i\rangle$  ( $i = 1, 2, 3$ ) which are the eigenstates of  $\hat{H}_{\text{vac}}$ . In the latter basis  $\hat{H}_{\text{vac}}$  is — up to a term proportional to the identity matrix — equal to

$$H_{\text{vac}}^{(\text{v})} = \frac{1}{2E} \text{diag}[m_1^2, m_2^2, m_3^2], \quad (2)$$

where the elements of  $H_{\text{vac}}^{(\text{v})}$  are defined as  $(H_{\text{vac}}^{(\text{v})})_{ij} \equiv \langle \nu_i | \hat{H}_{\text{vac}} | \nu_j \rangle$ , superscript “(v)” stands for the vacuum mass basis,  $E = |\mathbf{p}|$  is the energy of the neutrino, and  $m_i$  is the mass of  $\nu_i$ . The two bases are related by a unitary transformation

$$|\nu_{\alpha}\rangle = \sum_i U_{\alpha i}^* |\nu_i\rangle. \quad (3)$$

The unitary matrix  $U$  in equation (3) is conventionally parametrised with three vacuum mixing angles  $\theta_{12}$ ,  $\theta_{23}$  and  $\theta_{13}$ , and the three remaining phases  $\delta$ ,  $\alpha_1$  and  $\alpha_2$  ([Amsler et al, 2008](#)) as:

$$U = \begin{bmatrix} c_{12}c_{13} & s_{12}c_{13} & s_{13}e^{-i\delta} \\ -s_{12}c_{23} - c_{12}s_{23}s_{13}e^{i\delta} & c_{12}c_{23} - s_{12}s_{23}s_{13}e^{i\delta} & s_{23}c_{13} \\ s_{12}s_{23} - c_{12}c_{23}s_{13}e^{i\delta} & -c_{12}s_{23} - s_{12}c_{23}s_{13}e^{i\delta} & c_{23}c_{13} \end{bmatrix} \\ \times \text{diag}[e^{i\alpha_1/2}, e^{i\alpha_2/2}, 1], \quad (4)$$

where  $c_{ij} = \cos \theta_{ij}$  and  $s_{ij} = \sin \theta_{ij}$ . We will ignore the two Majorana phases  $\alpha_1$  and  $\alpha_2$  from this point because they have no effect for flavour transformation of ultra-relativistic neutrinos in matter (e.g. [Strumia and Vissani, 2006](#)). Various neutrino oscillation experiments have measured or put constraints on most of the neutrino mixing parameters:  $\delta m_{12}^2 = m_2^2 - m_1^2 \simeq \delta m_{\odot}^2 \simeq 8 \times 10^{-5} \text{ eV}^2$ ,  $|\delta m_{23}^2| = |m_3^2 - m_2^2| \simeq \delta m_{\text{atm}}^2 \simeq 2.4 \times 10^{-3} \text{ eV}^2$ ,  $\sin^2 2\theta_{12} \simeq 0.86$ ,  $\sin^2 2\theta_{23} \simeq 1$  and  $\sin^2 2\theta_{13} \lesssim 0.19$  ([Fogli et al, 2006b](#)). The  $CP$  phase  $\delta$  and the sign of  $\delta m_{23}^2$  are undetermined. It is conventional to call a mixing scheme a normal mass hierarchy if  $\delta m_{23}^2 > 0$  and an inverted mass hierarchy if  $\delta m_{23}^2 < 0$ .

The Hamiltonian  $\hat{H}_{\text{matt}}(\mathbf{r})$  is a diagonal matrix in the flavour basis

$$H_{\text{matt}}^{(\text{f})}(\mathbf{r}) = \text{diag}[V_e(\mathbf{r}), 0, 0] = \sqrt{2}G_{\text{F}}N_{\text{A}}\rho(\mathbf{r}) \text{diag}[Y_e(\mathbf{r}), 0, 0], \quad (5)$$

where superscript “(f)” denotes the flavour basis,  $G_{\text{F}} \simeq 1.166 \times 10^{-5} \text{ GeV}^{-2}$  is Fermi’s constant,  $N_{\text{A}} \simeq 6.022 \times 10^{23} \text{ g}^{-1}$  is Avogadro’s number,  $\rho(\mathbf{r})$  is the matter density, and  $Y_e(\mathbf{r})$  is the electron fraction per baryon. We note that the matter temperature outside the neutrino sphere is too low to have  $\mu$  or  $\tau$  produced. (However, see, e.g. [Dighe and](#)

Smirnov, 2000; Esteban-Pretel *et al*, 2008b for the effects of nonzero “effective”  $\mu$ -abundance in the presence of a very large matter density.) The eigenstates  $|\nu_i^m(\mathbf{r})\rangle$  ( $i = 1, 2, 3$ ) of the Hamiltonian  $\hat{H}(\mathbf{r}) = \hat{H}_{\text{vac}} + \hat{H}_{\text{matt}}(\mathbf{r})$  constitute the “matter basis”. We define matter eigenstates  $|\nu_i^m(\mathbf{r})\rangle$  to be in the same order as that of vacuum mass eigenstates  $|\nu_i\rangle$ , i.e. the eigenvalues  $k_i(\mathbf{r})$  associated with  $|\nu_i^m(\mathbf{r})\rangle$  satisfy  $k_1(\mathbf{r}) < k_2(\mathbf{r}) < k_3(\mathbf{r})$  for the normal mass hierarchy and  $k_3(\mathbf{r}) < k_1(\mathbf{r}) < k_2(\mathbf{r})$  for the inverted mass hierarchy. Unlike the flavour or vacuum mass states, the eigenstates  $|\nu_i^m(\mathbf{r})\rangle$  as well as the corresponding eigenvalues  $k_i(\mathbf{r})$  vary with location as the electron number density  $n_e(\mathbf{r}) = N_A \rho(\mathbf{r}) Y_e(\mathbf{r})$  changes. All the above discussions also apply to antineutrinos except that there is a sign difference between  $\hat{H}_{\text{matt}}(\mathbf{r})$  for neutrinos and for antineutrinos, i.e. one should take  $V_e(\mathbf{r}) \rightarrow -V_e(\mathbf{r})$  in equation (5) for antineutrinos.

As an alternative to solving equation (1) the evolution of a neutrino can also be found by solving for the evolution operator  $\hat{S}_{\mathbf{p}}(\mathbf{r}, \mathbf{r}_0)$ . This operator obeys a similar equation,

$$i \frac{d}{d\lambda} \hat{S}_{\mathbf{p}}(\mathbf{r}, \mathbf{r}_0) = \hat{H}(\mathbf{r}) \hat{S}_{\mathbf{p}}(\mathbf{r}, \mathbf{r}_0). \quad (6)$$

and has the additional property that it obeys the product rule:

$$\hat{S}_{\mathbf{p}}(\mathbf{r}, \mathbf{r}_0) = \hat{S}_{\mathbf{p}}(\mathbf{r}, \mathbf{r}') \hat{S}_{\mathbf{p}}(\mathbf{r}', \mathbf{r}_0). \quad (7)$$

Equation (6) has a formal solution

$$\hat{S}_{\mathbf{p}}(\mathbf{r}, \mathbf{r}_0) = \mathbb{T} \exp \left[ -i \int_{\lambda_0}^{\lambda} \hat{H}(\mathbf{r}') d\lambda' \right], \quad (8)$$

where  $\mathbb{T}$  is the space/time-ordering operator, and  $\lambda_0$ ,  $\lambda$  and  $\lambda'$  are the distances along the world line of the neutrino that correspond to  $\mathbf{r}_0$ ,  $\mathbf{r}$  and  $\mathbf{r}'$ , respectively. In practice,  $\hat{S}_{\mathbf{p}}(\mathbf{r}, \mathbf{r}_0)$  is approximated by a sum of truncated series (Kneller and McLaughlin, 2006; Kneller and McLaughlin, 2009).

## 2.2. The two-flavour approximation

We have, so far, described everything in terms of three flavours but a quick scan through the literature by the reader will reveal that many studies have used only two. The reduction in number of flavours comes from observation of how neutrinos evolve in the matter basis. The evolution operator  $\hat{S}_{\mathbf{p}}$  in this basis is a diagonal matrix and the probability for the neutrino to be in each matter eigenstate is constant except in the vicinity of the resonant regions where two of the three eigenvalues  $k_i$  of  $\hat{H}$  approach one another. The evolution of the eigenvalues as a function of the potential is shown in figure 2 and from it we see that there are two resonances: the “H” resonance at a larger matter density associated with the  $\delta m_{\text{atm}}^2$ -scale, and the resonance at the  $\delta m_{\odot}^2$ -scale known as the “L” resonance which occurs at a smaller matter density. As a result of the large difference between the two measured mass-squared differences,  $\delta m_{\odot}^2$  and  $\delta m_{\text{atm}}^2$ , neutrino mixing at any resonant location occurs principally between the two matter states whose eigenvalues are the closest, and the third matter state remains decoupled (Dighe and Smirnov, 2000; Kuo and Pantaleone, 1989b). Therefore, the full three-flavour mixing problem can be approximated as two successive two-flavour mixing scenarios that occur at the H and L resonances, respectively. Here the L resonance always describes the mixing between  $|\nu_1^m(\mathbf{r})\rangle$  and  $|\nu_2^m(\mathbf{r})\rangle$  but for the H resonance

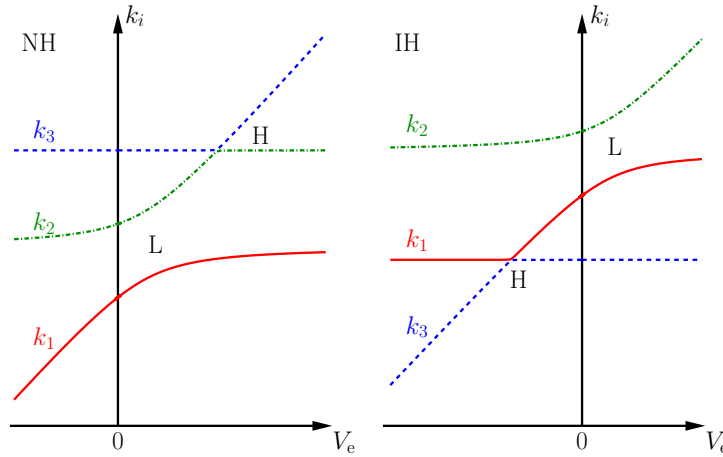


**Figure 2.** Schematic plots of  $k_i$ , the eigenvalues of Hamiltonian  $\hat{H}$ , as functions of  $V_e$  for the normal neutrino mass hierarchy (NH, the left panel) and the inverted neutrino mass hierarchy (IH, the right panel), respectively. The “H” and “L” MSW resonances are labelled correspondingly. The resonances occur at  $V_e > 0$  and  $V_e < 0$  are for neutrinos and antineutrinos, respectively. The eigenvalues of the two distinct matter states that are involved in the H resonance are close to each other (but do not equal) at the resonance.

the mixing states differ being  $|\nu_2^m(\mathbf{r})\rangle$  and  $|\nu_3^m(\mathbf{r})\rangle$  for normal mass hierarchy and the states  $|\bar{\nu}_1^m(\mathbf{r})\rangle$  and  $|\bar{\nu}_3^m(\mathbf{r})\rangle$  for inverted mass hierarchy.

Either the H or L resonance is said to be “adiabatic” or “non-adiabatic” depending upon whether the crossing probability  $P_C$  is close to zero or closer to unity and indeed these are the two natural values. If the electron number density  $n_e = \rho Y_e$  has a power-law dependence on the distance along the world line of the neutrino, i.e.  $n_e(\lambda) \propto 1/(\lambda - \lambda_0)^n$ , the crossing probability  $P_C$  in the two-flavour approximation has an analytical solution

$$P_C = \exp\left(-\frac{\pi\gamma_\star F(n, \theta_\nu)}{2}\right). \quad (9)$$

In equation (9)

$$\gamma_\star = \sin^2 2\theta_\nu \frac{\delta m^2}{E^2} \left| \frac{dV_e(\mathbf{r})}{d\lambda} \right|_{\mathbf{r}=\mathbf{r}_\star}^{-1} \quad (10)$$

is the adiabaticity parameter evaluated at the resonant position  $\mathbf{r}_\star$  where

$$\frac{\delta m^2}{2E} \cos 2\theta_\nu - V_e(\mathbf{r}_\star) = 0. \quad (11)$$

Here  $\delta m^2$  and  $\theta_\nu$  are the mass-squared difference and effective vacuum mixing angle in the two-flavour approximation. The function  $F(n, \theta_\nu)$  in equation (9) depends solely on  $n$  and  $\theta_\nu$  and can be found in [Kuo and Pantaleone \(1989a\)](#) and [Kachelrieß and Tomàs \(2001\)](#). It is common to find authors using the Landau-Stückelberg-Zener ([Landau and Lifshitz, 1977](#); [Stückelberg, E. C. G., 1932](#); [Zener, 1932](#)) formula for a linear density profile for which  $F = 1$ .

When equation (9) is applied to the L resonance with  $\delta m^2 \simeq \delta m_\odot^2$  and  $\theta_\nu \simeq \theta_\odot$  it turns out that the crossing probability is always very small — as in the sun — and

the neutrino transformation is adiabatic (Dighe and Smirnov, 2000). As a result, one always has

$$S_{\mathbf{p}} \sim \begin{bmatrix} 1 & 0 & 0 \\ 0 & \alpha_{\text{H}} & \beta_{\text{H}} \\ 0 & -\beta_{\text{H}}^* & \alpha_{\text{H}}^* \end{bmatrix} \quad \text{and} \quad \bar{S}_{\mathbf{p}} \sim \begin{bmatrix} \bar{\alpha}_{\text{H}} & 0 & \bar{\beta}_{\text{H}} \\ 0 & 1 & 0 \\ -\bar{\beta}_{\text{H}}^* & 0 & \bar{\alpha}_{\text{H}}^* \end{bmatrix}, \quad (12)$$

where  $S_{\mathbf{p}}$  ( $\bar{S}_{\mathbf{p}}$ ) is the matrix of the evolution operator in the matter basis that evolves the neutrino from the neutrino sphere to the surface of the supernova, and “ $\sim$ ” means that the two matrices are different only by some diagonal matrices which do not change the probability for the neutrino or antineutrino to be in each matter eigenstate (Kneller *et al*, 2008). In equation (12)  $\alpha_{\text{H}}$  and  $\beta_{\text{H}}$  ( $\bar{\alpha}_{\text{H}}$  and  $\bar{\beta}_{\text{H}}$ ) are the Cayley-Klein parameters for  $S_{\text{H}}$  ( $\bar{S}_{\text{H}}$ ), the evolution operator in the matter basis that describes the two-flavour mixing scenario for the H resonance of the neutrino (antineutrino). Up to a common phase factor which is irrelevant for neutrino oscillations we can write

$$S_{\text{H}} = \begin{bmatrix} \alpha_{\text{H}} & \beta_{\text{H}} \\ -\beta_{\text{H}}^* & \alpha_{\text{H}}^* \end{bmatrix} \quad \text{and} \quad \bar{S}_{\text{H}} = \begin{bmatrix} \bar{\alpha}_{\text{H}} & \bar{\beta}_{\text{H}} \\ -\bar{\beta}_{\text{H}}^* & \bar{\alpha}_{\text{H}}^* \end{bmatrix}, \quad (13)$$

where the dependence of Cayley-Klein parameters on neutrino momentum is implicit. The Cayley-Klein parameters satisfy the unitary condition

$$|\alpha_{\text{H}}|^2 + |\beta_{\text{H}}|^2 = 1 \quad \text{and} \quad |\bar{\alpha}_{\text{H}}|^2 + |\bar{\beta}_{\text{H}}|^2 = 1. \quad (14)$$

From equations (13) and (14) we see that the crossing probability at the H resonance is

$$P_{\text{H}} = 1 - |\alpha_{\text{H}}|^2 = |\beta_{\text{H}}|^2 \quad (15)$$

for neutrinos and

$$\bar{P}_{\text{H}} = 1 - |\bar{\alpha}_{\text{H}}|^2 = |\bar{\beta}_{\text{H}}|^2 \quad (16)$$

for antineutrinos.

For the H resonance the appropriate substitutions into equation (11) are  $\theta_{\nu} \simeq \theta_{13}$  and  $\delta m^2 \simeq \pm \delta m_{\text{atm}}^2$ , where the plus and minus signs are for normal mass hierarchy and inverted mass hierarchy, respectively. But, as figure 2 illustrates, we cannot have a situation where an H resonance exists for both neutrinos *and* antineutrinos. For this reason we must have  $\bar{\beta}_{\text{H}} = 0$  for a normal hierarchy and  $\beta_{\text{H}} = 0$  for an inverted hierarchy .

### 2.3. Neutrino self-interaction potential

Assuming that the effects of the neutrino medium on the flavour evolution of a test neutrino depend on the average flavour content of background neutrinos (Balantekin and Pehlivan, 2007; Friedland and Lunardini, 2003a,b), Hamiltonian  $\hat{H}_{\nu\nu}$  for a neutrino with momentum  $\mathbf{p}$  can be written in the flavour basis as

$$H_{\nu\nu,\mathbf{p}}^{(\text{f})}(\mathbf{r}) = \sqrt{2}G_{\text{F}} \int \frac{d^3\mathbf{p}'}{(2\pi)^3} [1 - \cos\vartheta_{\mathbf{p}\mathbf{p}'}(\mathbf{r})][\varrho_{\nu,\mathbf{p}'}(\mathbf{r}) - \varrho_{\bar{\nu},\mathbf{p}'}^*(\mathbf{r})], \quad (17)$$

where  $\mathbf{p}$  and  $\mathbf{p}'$  are the momenta of the test and background neutrinos, respectively,  $\vartheta_{\mathbf{p}\mathbf{p}'}$  is angle between the propagation directions of these neutrinos, and  $\varrho_{\nu(\bar{\nu}),\mathbf{p}'}$  are the matrices of density describing the flavour states of background neutrinos (antineutrinos). (In Sigl and Raffelt (1993); Strack and Burrows (2005) the density of matrix for an antineutrino is actually defined as  $[\bar{\varrho}_{\mathbf{p}}(\mathbf{r})]_{\alpha\beta} = [\varrho_{\bar{\nu},\mathbf{p}}]_{\beta\alpha} = [\varrho_{\bar{\nu},\mathbf{p}}^*]_{\alpha\beta}$ . This definition of the density of matrix with a reversed order in subscripts is helpful if one

uses matrices of densities instead of wavefunctions to describe the flavour states of neutrinos. See equation (48) and discussions in section 4.2.) Note that we use  $\vartheta$  and  $\theta$  (with or without subscripts or superscripts) to denote angles that are in coordinate space and flavour space, respectively. Similarly, the Hamiltonian for an antineutrino with momentum  $\mathbf{p}$  is

$$\bar{H}_{\nu\nu,\mathbf{p}}^{(f)}(\mathbf{r}) = \sqrt{2}G_{\text{F}} \int \frac{d^3\mathbf{p}'}{(2\pi)^3} [1 - \cos\vartheta_{\mathbf{p}\mathbf{p}'}(\mathbf{r})][\varrho_{\bar{\nu},\mathbf{p}'}(\mathbf{r}) - \varrho_{\nu,\mathbf{p}'}^*(\mathbf{r})]. \quad (18)$$

Assuming that the flavour state of each neutrino can be fully described by a wavefunction (i.e. without any quantum decoherence), the elements of the matrices of densities for neutrinos and antineutrinos can be written as

$$[\varrho_{\nu,\mathbf{p}}(\mathbf{r})]_{\alpha\beta} = \sum_{\nu'_{\mathbf{p}}} F_{\nu'_{\mathbf{p}}}(\mathbf{r}) \langle \nu_{\alpha} | \psi_{\nu'_{\mathbf{p}}}(\mathbf{r}) \rangle \langle \psi_{\nu'_{\mathbf{p}}}(\mathbf{r}) | \nu_{\beta} \rangle, \quad (19)$$

$$[\varrho_{\bar{\nu},\mathbf{p}}(\mathbf{r})]_{\alpha\beta} = \sum_{\bar{\nu}'_{\mathbf{p}}} F_{\bar{\nu}'_{\mathbf{p}}}(\mathbf{r}) \langle \bar{\nu}_{\alpha} | \psi_{\bar{\nu}'_{\mathbf{p}}}(\mathbf{r}) \rangle \langle \psi_{\bar{\nu}'_{\mathbf{p}}}(\mathbf{r}) | \bar{\nu}_{\beta} \rangle, \quad (20)$$

where  $\nu'_{\mathbf{p}}$  ( $\bar{\nu}'_{\mathbf{p}}$ ) represents a neutrino (antineutrino) beam with momentum  $\mathbf{p}$ ,  $F_{\nu'_{\mathbf{p}}}(\bar{\nu}'_{\mathbf{p}})(\mathbf{r})$  is its number flux at  $\mathbf{r}$ , and  $|\psi_{\nu'_{\mathbf{p}}}(\bar{\nu}'_{\mathbf{p}})\rangle$  is the flavour state of the neutrino (antineutrino). The diagonal elements of a matrix of density give the number densities of neutrinos in the corresponding flavours. For example,

$$n_{\nu_e}^{\text{tot}}(\mathbf{r}) = \int \frac{d^3\mathbf{p}'}{(2\pi)^3} [\varrho_{\nu,\mathbf{p}'}(\mathbf{r})]_{ee} \quad (21)$$

is the total number density of  $\nu_e$  at  $\mathbf{r}$ . The off-diagonal elements of a matrix of density contain information about neutrino flavour mixing.

Like in pure MSW flavour transformation, the problem of three-flavour neutrino oscillation with neutrino self-interaction is also believed to be factorisable into two successive two-flavour mixing scenarios under most circumstances (Dasgupta and Dighe, 2008; Dasgupta *et al.*, 2008c; Duan *et al.*, 2008d). In this review will focus on the two-flavour mixing scenario at the  $\delta m_{\text{atm}}^2$ -scale which is the mostly likely neutrino mixing scenario to affect, if at all, supernova dynamics and/or nucleosynthesis.

### 3. Neutrino flavour transformation in supernovae: the electron dominated regime

In this section we review the effects of dynamical density profiles on flavour transformation of supernova neutrinos. In sections 3.1 and 3.2 we will discuss the effects of the forward and reverse shocks and hot bubbles. In doing so we will utilise density profiles that are derived from 1D supernova simulations and we will focus on neutrinos that are emitted radially from the PNS. In section 3.3 we will discuss the features in aspherical profiles and flavour transformation of neutrinos that propagate along non-radial trajectories.

#### 3.1. The forward shock

Until recently any study of supernova neutrino oscillations assumed the density profile observed by the outrushing neutrinos to be that of the progenitor star and to be static. Roughly this profile obeys an inverse power law i.e.  $\rho \propto 1/r^n$  with common values of  $n$  being 2–3 (Brown *et al.*, 1982; Dighe and Smirnov, 2000; Kuo and Pantaleone, 1988;

Nötzold, 1987) though upon closer inspection one finds that profiles of progenitors from simulations show deviations from this form (Kneller *et al*, 2008; Nötzold, 1987; Takahashi *et al*, 2003). Whatever progenitor profile used, we must first establish as a baseline the effect of the progenitor upon the neutrinos because, a) for the first second or so of the neutrino signal this is the profile at the H resonance, and b), it changes from this baseline that reveal the evolution of the density profile.

An insightful study of the effects of the progenitor was made by Lunardini and Smirnov (2003). Using equation (9) with the appropriate mixing parameters for the H resonance and adopting an inverse power law profile they distinguished three regimes in the parameter space of  $\theta_{13}$ :

- The adiabatic regime where

$$\sin^2 \theta_{13} \gtrsim 10^{-4} \left( \frac{E}{10 \text{ MeV}} \right)^{2/3}. \quad (22)$$

In this regime  $\gamma_* \gg 1$  and  $P_H \sim 0$  for the normal hierarchy or  $\bar{P}_H \sim 0$  for the inverted hierarchy.

- The non-adiabatic regime where

$$\sin^2 \theta_{13} \lesssim 10^{-6} \left( \frac{E}{10 \text{ MeV}} \right)^{2/3}. \quad (23)$$

In this regime  $\gamma_* \ll 1$  and  $P_H \sim 1$  (or  $\bar{P}_H \sim 1$ ).

- The transition regime where

$$\sin^2 \theta_{13} \sim (10^{-6} - 10^{-4}) \left( \frac{E}{10 \text{ MeV}} \right)^{2/3}. \quad (24)$$

In this regime  $\gamma_* \sim 1$  and  $P_H$  (or  $\bar{P}_H$ ) takes on intermediate values.

The most significant change in the study of the pure-MSW in supernovae over recent years has been the realisation that the profile seen by the neutrinos at later times is not the progenitor profile. It is now apparent that prominent features appear in the profile of the supernova that are not present in the progenitor and these features will affect the neutrinos. The first, generic feature of any supernova density profile is the forward shock. Snapshots of density profiles with solely this feature are shown in figure 3 which is taken from Kneller *et al* (2008). The origin of time  $t$  is taken to be the formation of the shock, an event often called the ‘‘bounce’’. Observationally the bounce would be indicated by the neutronisation burst which occurs a millisecond or so afterwards. Kneller *et al* (2008) mapped into a hydrodynamical code a spherically symmetric (1D) density profile resembling the state of the supernova approximately at the moment when the forward shock has stalled at  $r \sim 200$  km. The material between a 100 km gain radius and the stalled shock was heated in a fashion resembling neutrino energy deposition in order to revive the outward motion of the shock. By adjusting the energy deposition rate Kneller *et al* (2008) could control the features of the explosion. We should mention that density profiles that *only* contain a forward shock are not typical of iron core-collapse supernova, nevertheless, such a simple profile is a useful place to begin to understand the manner in which the explosion affects the neutrinos. In the figure the forward shock is the step in density and we can see it racing out through the supernova and through the H resonances. For normal shocks the density

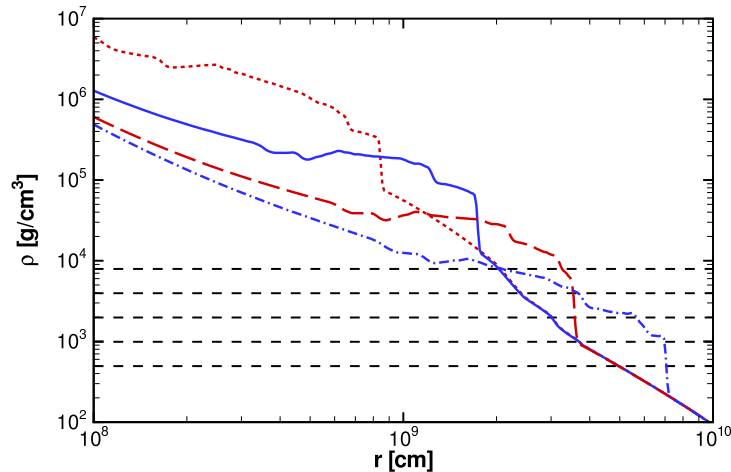


**Figure 3.** The density profile of a weak explosion in a spherically symmetric simulation taken from [Kneller et al \(2008\)](#). Displayed are the radial profile at a series of snapshot times which are:  $t = 0.9$  s (dotted),  $1.8$  s (solid),  $3.6$  s (dashed) and  $7.2$  s (dash dot). The horizontal dashed lines are the H resonance densities of, from top to bottom, neutrinos with energies of 5, 10, 20, 40 and 80 MeV.

jump,  $\Delta\rho_{\text{sh}}/\rho_{\text{sh}}$ , is related to the Mach number,  $M$ , of the shock and the ratio of specific heats,  $C_P/C_V$ , of the medium via

$$\frac{\Delta\rho_{\text{sh}}}{\rho_{\text{sh}}} = \frac{2(M^2 - 1)}{(C_P/C_V - 1)M^2 + 2}. \quad (25)$$

For strong shocks the density jump becomes independent of the Mach number.

As the shock reaches the H resonance for any given neutrino energy the density derivative  $d\rho/dr$  becomes abruptly steeper. This will change the adiabaticity of the resonance according to equation (10). If the mixing parameters are such that neutrino propagation through the progenitor is adiabatic, i.e.  $\theta_{13}$  lies in the adiabatic regime so that  $P_H \sim 0$ , then the arrival of the shock at any given resonance means that neutrinos of the same energy now propagate through the profile non-adiabatically, i.e.  $P_H \sim 1$ . It is the possibility, first considered by [Schirato and Fuller \(2002\)](#), that  $P_H$  can evolve with time that allows us to peer inside the supernova as it explodes. Of course if  $\theta_{13}$  is very small so that it lies in the non-adiabatic regime then no change will be observed as the shock passes the H resonance region because the H resonance is already non-adiabatic for the undisturbed/progenitor profile, i.e.  $\gamma_* \ll 1$ ,  $P_H \sim 1$ . When the shock arrives all that happens is that  $\gamma_*$  will become even smaller and but this has no effect upon  $P_H$ . Such a situation would be disappointing but at least we would be able to set an upper limit on  $\theta_{13}$  that is competitive with any possible terrestrial experiment. So for the rest of this discussion of the dynamic MSW effect we shall consider only the case where  $\theta_{13}$  lies in the adiabatic regime, i.e.  $\theta_{13}$  is such that equation (22) is satisfied, and more specifically adopt a value  $\sin^2 2\theta_{13} = 4 \times 10^{-4}$ .

With our understanding of how  $P_H$  can change as the star explodes we can begin to map out our expectations for the evolution of  $P_H$  as a function of time and energy. Let us consider the particular example shown in figure 3. For the first couple of seconds the profile at the H resonances of neutrinos with energy 5 – 80 MeV is still

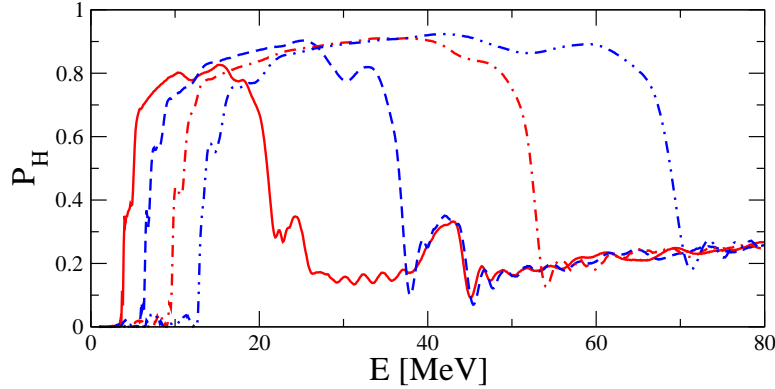


**Figure 4.** The crossing probability as a function of neutrino energy for a supernova simulation containing only a forward shock. Density profiles from this simulation are shown in figure 3 and the snapshot times are:  $t = 3.0$  s (solid),  $3.5$  s (dashed),  $4.0$  s (dash-dot) and  $4.5$  s (dash-double dot). The figure is taken from Kneller *et al* (2008).

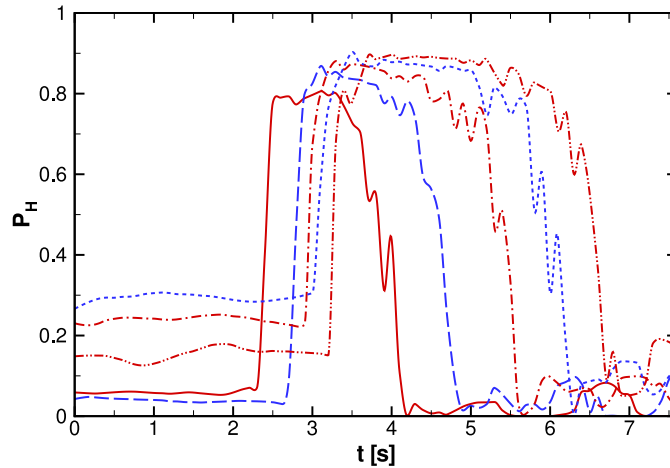


**Figure 5.** The crossing probability as a function of time for selected neutrino energies as they pass through the density profiles taken from the weak explosion shown in figure 3. The energies are:  $E = 10$  MeV (solid),  $15$  MeV (dashed),  $20$  MeV (dash dot),  $25$  MeV (dotted) and  $30$  MeV (dash double dot). The figure is taken from Kneller *et al* (2008).

the undisturbed progenitor and only after this initial delay does the shock appear in the H resonance region. Then at  $t = 2.0$  s the shock will change the adiabaticity of the  $5$  MeV neutrinos but will not begin to affect the  $40$  MeV neutrinos until later at  $3.6$  s because it takes longer for the shock to reach their H resonance density. Also around  $3.5$  s the shock ceases to intersect the  $5$  MeV resonance density so for this energy the adiabaticity will return to  $P_H \sim 0$ . Only later at  $t = 7.2$  s does the shock cease affecting the  $40$  MeV neutrinos.

In figures 4 and 5 we show the actual numerical results for the crossing probability



$P_H$  as a function of energy at various snapshot times, and as a function of time for fixed neutrino energies respectively as neutrinos pass through density profiles taken from the weak supernova shown in figure 3. We clearly see the arrival of the shock at early times as the sudden jump in  $P_H$  at low energies which then sweeps up through the spectrum. Note how the width of the shock feature increases with time. We also see that higher energy neutrinos are affected after the lower energies and that the effect is of longer duration as expected. From figures 4 and 5 we can identify three basic quantities that describe the evolution of  $P_H$ :

- $E_{\text{sh}}(t)$ , the highest energy affected by the shock at any given moment  $t$ ,
- $\Delta E_{\text{sh}}(t)$ , the width of the shock feature in the spectrum at any given  $t$ , and
- $\Delta t_{\text{sh}}(E)$ , the time period over which the shock affects neutrinos of energy  $E$ .

From figures 4 and 5 we see that both  $E_{\text{sh}}(t)$  and  $\Delta E_{\text{sh}}(t)$  increase with  $t$  and that  $\Delta t_{\text{sh}}(E)$  increases with  $E$ . This behaviour is easily understood.

The highest energy affected by the shock,  $E_{\text{sh}}(t)$ , at time  $t$  corresponds to the moment when the bottom of the shock reaches the resonance density for that particular energy as shown in figure 3.  $E_{\text{sh}}(t)$  is a monotonically increasing function of  $t$  which is a generic prediction and occurs simply because the resonance density is inversely proportional to the neutrino energy, the density profile is a monotonically decreasing function of distance and because the shock wave is generated at the core of the star where the density is highest.

The width of the shock feature,  $\Delta E_{\text{sh}}(t)$ , also monotonically increase with  $t$ . This can be understood as follows. The resonance condition (11) allows us to relate  $E_{\text{sh}}(t)$  to the value of the neutrino potential at the bottom of the shock,  $V_{\text{sh}}(t)$ , by

$$V_{\text{sh}} = \frac{\delta m^2 \cos 2\theta_{\nu}}{2 E_{\text{sh}}}. \quad (26)$$

The lowest energy affected by the shock,  $E_{\text{sh}} - \Delta E_{\text{sh}}$  are those neutrinos whose resonance density is the top of the shock, i.e.  $V_{\text{sh}} + \Delta V_{\text{sh}}$  where  $\Delta V_{\text{sh}}$  is the jump in the neutrino potential across the shock. Using equation (26) and exploiting the fact that  $\Delta V_{\text{sh}}/V_{\text{sh}} = \Delta \rho_{\text{sh}}/\rho_{\text{sh}}$  — where  $\rho_{\text{sh}}(t)$  is the density at the bottom of the shock and  $\Delta \rho_{\text{sh}}(t)$  the density jump — we can derive the simple relationship that

$$\frac{\Delta E_{\text{sh}}}{E_{\text{sh}} - \Delta E_{\text{sh}}} = \frac{\Delta \rho_{\text{sh}}}{\rho_{\text{sh}}}. \quad (27)$$

Note that this is independent of the mixing parameters. If the ratio of specific heats of the material does not change rapidly with distance then  $\Delta \rho_{\text{sh}}/\rho_{\text{sh}}$  is constant for a strong shock — equation (25) — so the ratio  $\Delta E_{\text{sh}}/(E_{\text{sh}} - \Delta E_{\text{sh}})$  is also invariant. This relationship shows us that  $\Delta E_{\text{sh}} \propto E_{\text{sh}}$ . Thus, if  $E_{\text{sh}}$  monotonically increases with  $t$  then so must  $\Delta E_{\text{sh}}$ .

Finally, that  $\Delta t_{\text{sh}}(E)$  increases with  $E$  is also just a consequence of  $E_{\text{sh}}$  increasing with  $t$ . The density  $\rho_{\text{sh}}(t)$  is the point where the shock attaches to the progenitor profile so if we assume a form for the density profile of the progenitor then we can relate  $\rho_{\text{sh}}(t)$  to the position of the shock,  $r_{\text{sh}}(t)$ . For illustrative purposes we shall adopt for the profile the power law  $\rho = C_{\star} (r_{\star}/r)^n$  with  $C_{\star}$  the constant of proportionality and  $r_{\star}$  some scale but it is possible to do better if the progenitor star can be identified. Using the adopted profile we find that  $E_{\text{sh}}$  is related to the shock radius by

$$r_{\text{sh}} = r_{\star} \left( \frac{\sqrt{8} G_{\text{F}} Y_e C_{\star} E_{\text{sh}}}{m_N \delta m^2 \cos 2\theta_{\nu}} \right)^{1/n}. \quad (28)$$

At a time  $t'$  the shock will have moved outwards through the star and will be located at a position  $r'_{\text{sh}} = r_{\text{sh}}(t')$ . As it does so the shock feature will have swept up through the neutrino spectrum with  $E'_{\text{sh}} = E_{\text{sh}}(t')$  now the highest affected energy and the spectral width will now be  $\Delta E'_{\text{sh}} = \Delta E_{\text{sh}}(t')$ . From equation (28) we see that  $r_{\text{sh}}/r'_{\text{sh}} = (Y_e E_{\text{sh}}/Y'_e E'_{\text{sh}})^{1/n}$  where  $Y'_e$  is the electron fraction at  $r'_{\text{sh}}$ . If we select  $t'$  to be the moment when neutrinos of energy  $E_{\text{sh}}$  cease to be affected by the shock then we must have  $E_{\text{sh}} = E'_{\text{sh}} - \Delta E'_{\text{sh}}$ . The time difference  $t' - t = \Delta t(E_{\text{sh}})$ . If  $\bar{v}_{\text{sh}}$  is the average shock velocity over this time period then we can derive that

$$\Delta t(E_{\text{sh}}) = \frac{r'_{\text{sh}} - r_{\text{sh}}}{\bar{v}_{\text{sh}}} = \frac{r'_{\text{sh}}}{\bar{v}_{\text{sh}}} \left[ \left( \frac{E'_{\text{sh}}}{E'_{\text{sh}} - \Delta E'_{\text{sh}}} \right)^{1/n} \left( \frac{Y'_e}{Y_e} \right)^{1/n} - 1 \right]. \quad (29)$$

The term in square brackets is a constant for a constant  $\Delta\rho_{\text{sh}}/\rho_{\text{sh}}$  and a medium with constant  $Y_e$  thus  $\Delta t(E_{\text{sh}})$  is proportional to  $r'_{\text{sh}}$ . With this discovery we immediately see that if  $r_{\text{sh}}$  increases with  $E_{\text{sh}}$ , so must  $\Delta t(E_{\text{sh}})$  increase with  $E_{\text{sh}}$ .

While equation (29) shows us that  $\Delta t(E_{\text{sh}})$  must increase with  $E_{\text{sh}}$  perhaps what is more interesting is that we can turn the equation around and use the observations of  $E_{\text{sh}}(t)$ ,  $\Delta E_{\text{sh}}(t)$ , and  $\Delta t_{\text{sh}}(E)$  to determine the average velocity of the shock as it travelled from  $r_{\text{sh}}$  to  $r'_{\text{sh}}$ ; that is

$$\bar{v}_{\text{sh}} = \frac{r_{\text{sh}}(E_{\text{sh}})}{\Delta t_{\text{sh}}(E_{\text{sh}})} \left[ \left( \frac{E'_{\text{sh}}}{E'_{\text{sh}} - \Delta E'_{\text{sh}}} \right)^{1/n} \left( \frac{Y'_e}{Y_e} \right)^{1/n} - 1 \right]. \quad (30)$$

As an alternative, we could simply exploit equation (28) to relate the observed  $E_{\text{sh}}(t)$  to construct  $r_{\text{sh}}(t)$  which can then be fit with a parametric form. The shock velocity would then be found as the derivative of  $r_{\text{sh}}(t)$  but there is additional information in the fit. The shock is formed at the PNS and current models of supernova indicate it stalls at  $r \sim 200$  km. Somehow the outward motion of the shock is revived and thereafter it races through the mantle of the supernova. The time spent by the shock in the stalled position is not known but suggestions typically lie in the range of  $\sim 0.5$  s. The velocity of the shock through the star is also not known but a reasonable initial guess is that the shock velocity is approximately constant because the profile is close to a  $1/r^3$  form (Sedov, 1959). Thus our expectation might be that the position of the shock after its revival is a simple linear model given by

$$r_{\text{sh}}(t) = r_{\text{stall}} + v_{\text{sh}}(t - t_{\text{stall}}) \quad (31)$$

where  $r_{\text{stall}}$  is the radius at which the shock stalls and  $t_{\text{stall}}$  is the time at which the shock was revived. The shock velocity  $v_{\text{sh}}$  is of course the gradient of equation (31) and the intercept is equal to  $r_{\text{stall}} - v_{\text{sh}} t_{\text{stall}}$ . So if we set  $r_{\text{stall}}$  to zero then we derive that  $t_{\text{stall}} = r_{\text{sh}}/v_{\text{sh}}$  and obtain the earliest time that the shock can have been revived. Thus, if the neutrino signal from the next Galactic supernova is of sufficient quality we might be able to determine a lower bound for  $t_{\text{stall}}$  and in doing so we would be able to confirm or refute a fundamental component of the core-collapse supernova paradigm: that the shock stalls and is revived.

### 3.2. Hot bubbles and reverse shocks

The density profiles of the supernova simulation used in the previous section were from a very weak supernova simulation and contained only a forward shock. The shock was revived by heating the material above the PNS but the energy deposition does not switch off once the forward shock has been revived but rather will continue for some

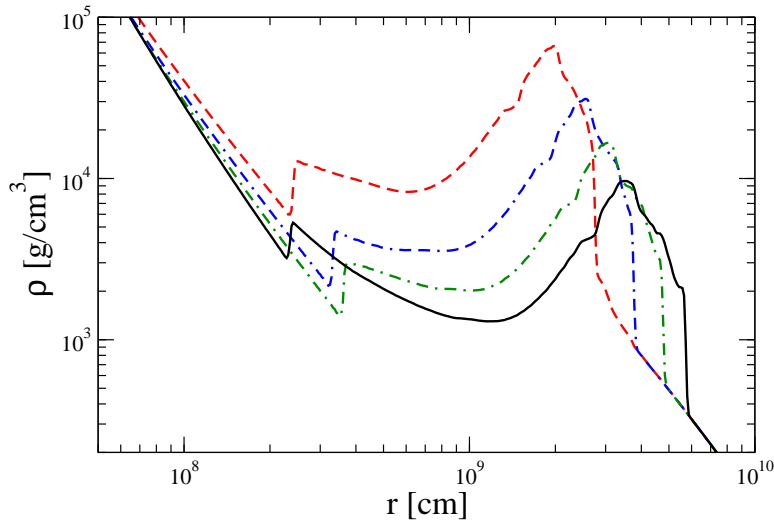


**Figure 6.** Density profiles containing a reverse shock. This figure is adapted from a figure in [Kneller \*et al\* \(2008\)](#). The snapshot times are:  $t = 1.5$  s (dashed), 2.0 s (dot double-dashed), 2.5 s (dot dashed) and 3.0 s (solid).

time after. The continued heating creates a wind that pushes outwards to create a hot bubble behind the forward shock. It was actually profiles of this type that were studied by [Schirato and Fuller \(2002\)](#). If we up the rate of energy deposition then strength of the wind can grow to the point where its velocity becomes greater than the sound speed. This situation leads to the formation of a second shock which faces the PNS rather than the exterior ([Burrows \*et al\*, 1995](#); [Janka and Mueller, 1995](#)), i.e. it is reversed compared to the forward shock. Profiles with reverse shocks are shown in figure 6. The behaviour of the reverse shock has been studied by [Tomàs \*et al\* \(2004\)](#), [Arcones \*et al\* \(2007\)](#) and [Kneller \*et al\* \(2008\)](#) in 1D and 2D using hydro codes of varying degrees of sophistication. It has been found that its behaviour is much richer than the forward shock due to its greater sensitivity to the mechanism by which it was formed, i.e. the energy deposition. If the heating is sustained for a long period then the reverse shock trails the forwards shock through the star, but if the energy deposition is over a briefer period then the reverse shock has been seen to diminish in size, stall and then to turn around and head back to the core. This can be seen in figure 6. Also we see from the figure how the densities either side of the reverse shock will change in relation to the forward shock as a function of time.

The hot bubble and the reverse shock also affect the neutrinos. If a profile contains either feature then we see that, at any given moment, there are some neutrino energies that will experience three (or more) resonances. In order to compute the effects of multiple resonance one must be careful less certain effects are ignored. Examples of calculations of  $P_H$  as a function of neutrino energy through supernova profiles containing reverse shocks are shown in figures 7 and 8. While some parts of figure 7 in particular resemble figure 4 we see also that something has noticeably changed. The crossing probability is seen to oscillate rapidly for some ranges of neutrino energies and the reason is due to “phase effects”. That phase effects are present in  $P_H$  for supernova profiles was first noticed by [Fogli \*et al\* \(2003\)](#). They were found again by

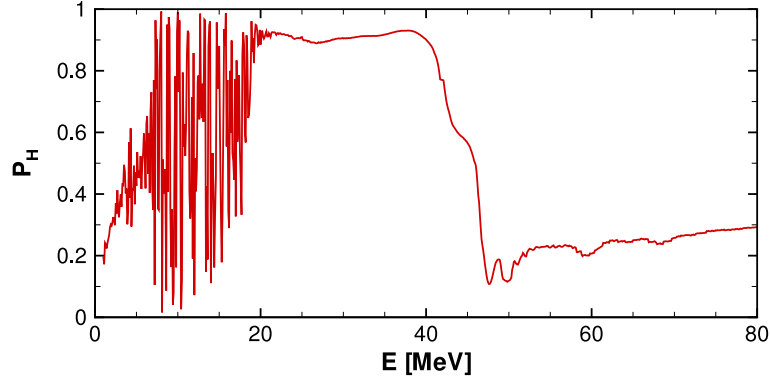


**Figure 7.** The crossing probability as a function of neutrino energy for a supernova simulation containing a reverse shock. Density profiles for this simulation are shown in figure 6. The snapshot time is  $t = 2.0$  s and the energy resolution is 100 keV. The figure is adapted from Kneller *et al* (2008) and corresponds to the 1D model with a total energy deposition  $Q = 3.36 \times 10^{51}$  erg.

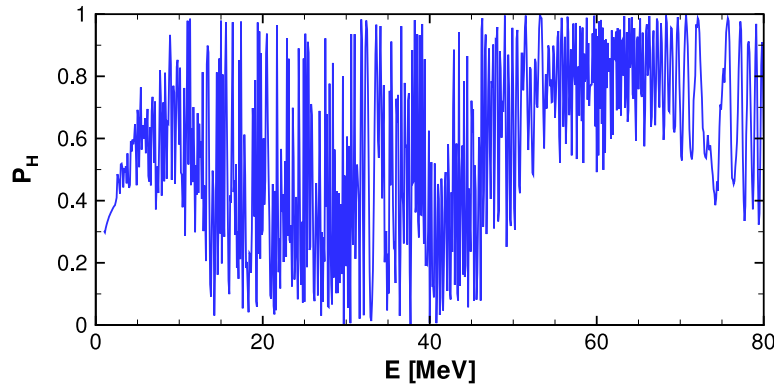


**Figure 8.** The crossing probability as a function of neutrino energy for a supernova simulation containing a reverse shock. Density profiles from this simulation are shown in Kneller *et al* (2008) and correspond to the model where the total energy deposition is  $Q = 4.51 \times 10^{51}$  erg. The snapshot time is  $t = 2.0$  s and the energy resolution is 100 keV.

Kneller and McLaughlin (2006) who also presented some basic arguments for why the phase effects appear. The phase effects and their detectability were then the focus of Dasgupta and Dighe (2007).

While, perhaps, initially surprising the origin of the phase effects is quite simple. The neutrino wavefunction after passing through multiple H resonances is  $\psi(r_*) = S_H(r_*, R_\nu)\psi(R_\nu)$  where  $r_*$  is some point between the H resonances and the L resonance, and  $R_\nu$  is the radius of the neutrino sphere. We can factorise  $S_H$  by dividing up the profile into regions within which there is just one H resonance, i.e. just one location in each region where equation (11) is satisfied. Using the product rule, equation (7),  $S_H$  is the product of evolution operators over the sub-domains:  $S_H = \dots S_{H2} S_{H1}$  where  $S_{Hi}$  is the  $S$  matrix for passage through the  $i$ 'th H resonance

encountered by the neutrino. All these  $S_{Hi}$  matrices, up to a phase which is irrelevant for neutrino oscillations, have the same structure in the two flavour approximation,

$$S_{Hi} = \begin{bmatrix} \alpha_{Hi} & \beta_{Hi} \\ -\beta_{Hi}^* & \alpha_{Hi}^* \end{bmatrix} \quad (32)$$

where  $\alpha_{Hi}$  and  $\beta_{Hi}$  are, again, Cayley-Klein parameters. The crossing probability for the  $i$ 'th resonance is  $P_{Hi} = |\beta_{Hi}|^2 = 1 - |\alpha_{Hi}|^2$ . Even for the case of three H resonances we obtain a long and complicated expression for the net effect of the multiple resonances so to keep things simple we shall consider the example of just two resonances. In this case the net H resonance crossing probability,  $P_H$ , is just

$$P_H = P_{H2}(1 - P_{H1}) + (1 - P_{H2})P_{H1} + 2\Re(\alpha_{H1}\alpha_{H2}\beta_{H1}\beta_{H2}^*) \quad (33)$$

$$= P_2(1 - P_1) + (1 - P_2)P_1 + 2\sqrt{P_1P_2(1 - P_1)(1 - P_2)}\cos\phi_H \quad (34)$$

where  $\phi_H$  is a phase formed from the phases of the  $\alpha$ 's and  $\beta$ 's. The first two terms are what we would expect if there were no correlations; the last term represents interference and depends upon the relative phases of the  $\alpha$ 's and  $\beta$ 's, hence the name ‘‘phase effects’’. Note the amplitude of the oscillatory term is always smaller than the constant and maximal when  $P_{H1} = P_{H2} = 1/2$ . From this result we can begin to understand the results of Tomàs *et al* (2004) for profiles containing both reverse and forward shocks. The net effect upon the neutrinos of a given energy depends upon the relationship between the shocks and the resonance density. If the two shocks intersect completely different resonance densities then we have a situation where, at most, either  $|\beta_1| = 1$  or  $|\beta_2| = 1$  but not both. But if we have a case where the two shocks affect the same resonance densities then we can have a situation where  $|\beta_1| = |\beta_2| = 1$  and the two non-adiabatic transitions cancel. As we see in figure 6, the two shocks do not always overlap completely and so, due to the relative proportions of the forward and reverse shocks, the cancellation may be over just a limited range of neutrino energies while energies slightly larger or smaller may experience just one shock. This can create what Tomàs *et al* (2004) referred to as the ‘‘double dip’’ in the crossing probability  $P_H$ .

But in the more general case with many H resonances some of which are neither exactly adiabatic nor non-adiabatic we must consider the effect of the oscillatory terms such as the one in equation (34). Dasgupta and Dighe (2007) show that the phase  $\phi_H$  appearing in equation (34) is approximately

$$\phi_H(E) \approx \int_{r_{H1}(E)}^{r_{H2}(E)} \sqrt{\left(\frac{\delta m^2 \cos 2\theta_v}{2E} - 2V_e(r)\right)^2 + \left(\frac{\delta m^2 \sin 2\theta_v}{2E}\right)^2} dr. \quad (35)$$

where the  $r_{Hi}(E)$  are the (energy dependent) positions of the resonances i.e. those locations that satisfy equation (11). Equation (35) is just the integral of the difference between the eigenvalues over the distance between the two resonances. In order to compute it properly one needs the density profile  $V_e(r)$  but for our purposes we approximate the result by neglecting the first term under the square root since we are in the vicinity of the resonances where this term vanishes. Thus  $\phi_H$  is approximately

$$\phi_H \approx \frac{|\delta m^2| \sin 2\theta_v L_H}{2E} \quad (36)$$

where  $L_H = r_{H2} - r_{H1}$  is the distance between the resonances. Typically this distance is much greater than the wavelength of the oscillations ( $\sim E/\delta m^2 \sin 2\theta_v$ ), so that  $\phi_H$

is a large number ( $\phi_H \gg 1$ ). Now let us consider a change in  $E$  and/or  $L_H$ . The resulting phase change  $\delta\phi_H$  is

$$\delta\phi_H = \phi_H \left[ \frac{\delta L_H}{L_H} - \frac{\delta E}{E} \right]. \quad (37)$$

We require just a change  $\delta\phi_H = 2\pi$  in order for the oscillatory term in equation (34) to cycle through one period. If  $\phi_H$  is large, say  $\phi_H \sim 10^3$ , then a fractional change in the energy of just  $\delta E/E \sim 10^{-3}$  is enough to give us  $\delta\phi_H \sim 2\pi$ . For neutrinos with energy  $E \sim 10$  MeV we see that  $P_H$  will cycle over one period with a change of energy of just  $\delta E \sim 10$  keV.

From our understanding of equation (34) we can begin to digest the results for  $P_H$  as a function of neutrino energy shown in figure 7 and 8. In the first figure we again observe the presence of the forward shock in the spectrum because the crossing probability makes the transition from adiabatic to non-adiabatic propagation at  $E \sim 50$  MeV but in this same figure we also see that below  $E \sim 20$  MeV the crossing probability starts to oscillate as a function of  $E$ : this occurs because those energies now passes through multiple H resonances and so phase effects appear. In figure 8 phase effects dominate the entire spectrum. In both cases the oscillations are very rapid which is simply an indication that the resonances are spaced by a large number of oscillation wavelengths.

### 3.3. Aspherical and turbulent profiles

As we indicated back in section 1 there is now ample evidence that supernovae are aspherical and there has been significant recent progress in identifying what processes may be the root of the asphericity. The standing accretion shock instability was found by Blondin *et al* (2003) to generate large dipolar and quadrapolar modes from small perturbations of a stalled, spherical accretion shock. When the simulations were repeated in three-dimensional (3D) differential, post-shock flow was found indicating the “spinning up” the PNS (Blondin, 2005). More recent work (Blondin and Mezzacappa, 2006, 2007; Blondin and Shaw, 2007; Iwakami *et al*, 2008; Ohnishi *et al*, 2008; Scheck *et al*, 2006) have confirmed the result and furthered the understanding of the SASI.

As an example of an aspherical density profile we show in figure 9 a snapshot, taken from Kneller *et al* (2008), of an aspherical explosion. For this calculation the same “initial” density profile used in 1D was mapped into a 2D hydrodynamical code and heated to revive the motion of the forward shock. The total energy deposition was  $Q \approx 3 \times 10^{51}$  erg, the canonical explosion energy for the matter portion of the supernova. To generate the asphericity the heating was inhomogeneous with preferential energy deposition along the equator. From the figure we see that the density profile along each line of sight can be very different but within the density profile along any given radial slice we can still identify the forward and reverse shocks and a hot bubble region between them. The radial positions of the two shocks now depends upon the polar angle  $\vartheta$ . Upon closer inspection we find even in 2D that the reverse shock also abates and moves back to the core. Superimposed upon the generic template are “fluctuations” generated by more shocks, localised bubbles, sound waves, etc.

Snapshots of  $P_H$  as a function of neutrino energy are shown in figure 10. The transition from the progenitor profile to the forward shock appears once again as the

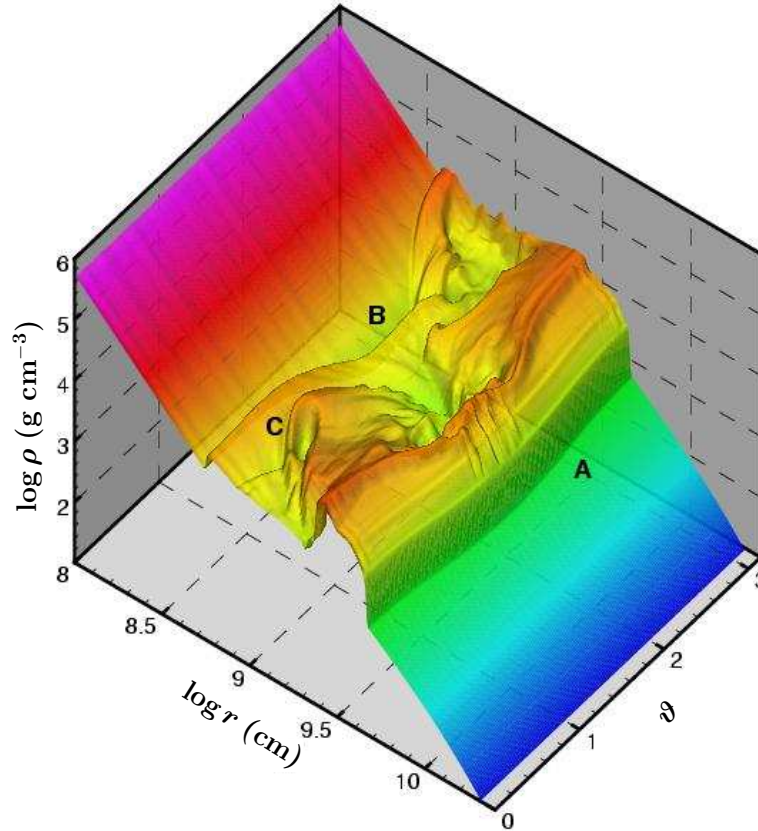


**Figure 9.** The density as a function of the radius and angle in a 2D supernova model at  $t = 2.5$  s taken from Kneller *et al* (2008). The forward shock is located to the left of “A”, the reverse shock is the step-up in density found to the right of “B”, and one of the many localised features in the profile is to the right of “C”.

transition to  $P_H \sim 1$  and we also notice how  $P_H$  drops suddenly around  $E \sim 10$  MeV for  $t = 2.4$  s when the profile becomes adiabatic again. Below  $E \sim 10$  MeV phase effects appear as the profile develops multiple resonances for these neutrino energies. Given the complexity of these profiles and our understanding of how multiple resonances affect neutrinos it comes as little surprise then that phase effects are prominent. By  $t = 5.4$  s they dominate the entire spectrum above 20 MeV. After  $t = 6.4$  s the forward shock, hot bubble, etc. have largely swept through the spectrum and we are able to notice a narrow range of energies surrounding  $E \sim 15$  MeV where phase effects again appear moving down through the spectrum. This is the signature of the reverse shock returning to the core.

The crossing probabilities shown in figure 10 are very similar to those shown earlier in figures 7 and 8. After comparing figure 10 with those figures one has a sense that the phase effects are somewhat stronger in 2D. In fact the phase effects are so strong that the crossing probability over wide swathes of the neutrino energy range appears to be essentially random with, more-or-less, uniform distribution from zero to unity. This impression of the uniformity of the distribution of  $P_H$  is confirmed by figure 11 where we plot the histogram of  $P_H$  from the middle panel of figure 10 for

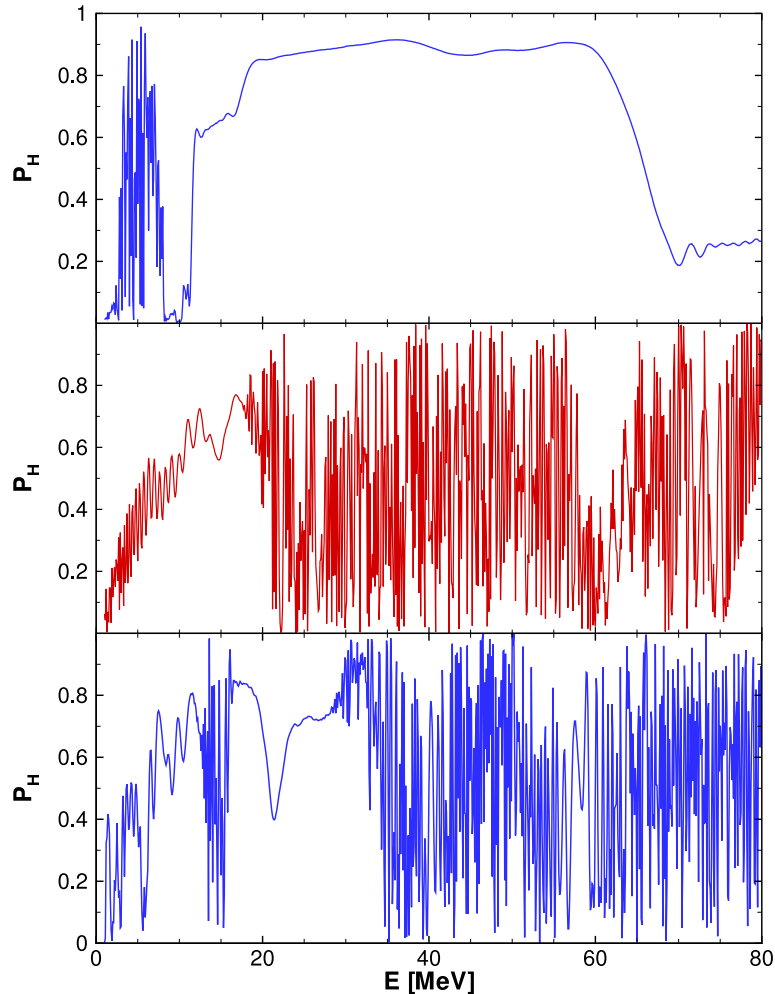


**Figure 10.** The H resonance crossing probability  $P_H$  as a function of neutrino energy for a radial slice at  $\vartheta = 25^\circ$  through the 2D supernova model. From top to bottom the snapshot times are  $t = 2.4$  s, 5.4 s and 6.4 s. The figure is taken from [Kneller \*et al\* \(2008\)](#).

neutrino energies between 30 MeV and 80 MeV. While not proof, figure 11 hints that the density profiles from 2D supernova simulations may cross over into the regime of turbulence. The effects upon neutrinos of a turbulent, noisy, density profile either in general or upon the solar density profile date back to [Schafer and Koonin \(1987\)](#), [Krastev and Smirnov \(1989\)](#), [Sawyer \(1990\)](#), [Loreti and Balantekin \(1994\)](#), [Balantekin \*et al\* \(1996\)](#) and many others thereafter. Turbulence in supernova was first considered by [Loreti \*et al\* \(1995\)](#) and then later by [Fogli \*et al\* \(2006a\)](#) in light of the fact that the evolving density profile was found to leave its imprint on the neutrino signal. In both cases  $\delta$ -correlated density fluctuations were assumed. More recently [Friedland and Gruzinov \(2006\)](#) and [Choubey \*et al\* \(2007\)](#) have used Kolmogorov fluctuation spectra. Whatever the fluctuation spectra used the same result emerges: if the turbulence is



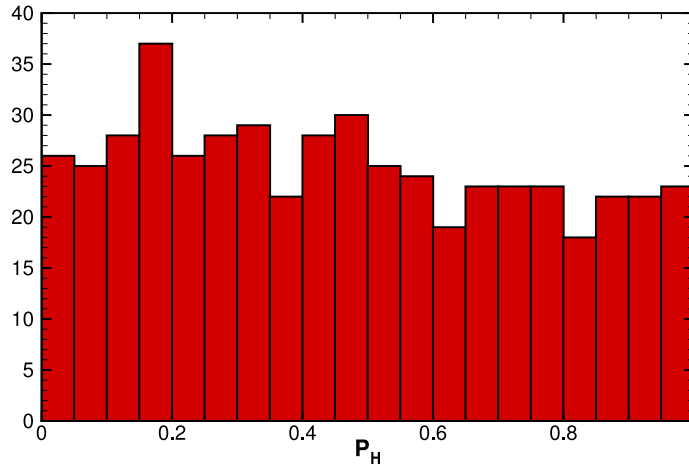


**Figure 11.** A histogram of  $P_H$  for neutrino energies between 30 and 80 MeV for neutrinos passing through the  $t = 5.4$  density profile shown in figure 10. The histogram is formed from 501 points and there are 20 bins so a uniform distribution would give an average count of 25 in each bin.

strong then  $P_H$  becomes a random variate uniformly distributed over the range  $[0, 1]$ . While this prediction seems to be in general agreement with figure 11 we remind the reader that what is plotted is the histogram of  $P_H$  for different neutrino energies at one snapshot time which is something different. For Fogli *et al* (2006a) fluctuations were restricted to a scale of less than 10 km while the spectra used by Friedland and Gruzinov (2006) permitted fluctuations on much larger scales. Friedland and Gruzinov (2006) showed that it is the density fluctuations on the scale of the oscillation wavelength at the resonances that contribute most and that the amplitude of the density fluctuations need only be greater than  $\delta\rho/\rho \gtrsim 0.1(\theta_{13})^{1/3}$  in order to enter the strong turbulence limit. For the value of  $\theta_{13}$  used when computing the results in figure 10 we require fluctuations of just  $\sim 1\%$  to reach this limit so indeed turbulence should be expected. Detecting turbulence in a neutrino signature would be a clear signature that the supernova exploded aspherically but one must not forget that we shall receive this signal along just one line of sight which makes demonstrating that the signal is the result of turbulence quite difficult.

#### 4. Neutrino flavour transformation in supernovae: effects of neutrino self-interaction

In this section we review neutrino oscillations with neutrino self-interaction in supernovae. For lack of space, we will focus on the key results of the two-flavour numerical simulations of supernova neutrino oscillations by Duan *et al* (2006a,b) and the analytical explanations of the results obtained under the single-angle approximation. In section 4.1 we describe in detail the two major approximations, i.e. the single-angle and multi-angle approximations, that are now employed to treat neutrino oscillations with neutrino self-interaction in supernovae. We also highlight the key results in the numerical simulations carried out by Duan *et al* (2006a,b). The

Schrödinger-like equation that governs neutrino flavour transformation, although well suited for studying flavour evolution of a single neutrino, is inconvenient when the neutrino potential  $\hat{H}_{\nu\nu}$  is not negligible. In section 4.2 we introduce the “language”, the notation of neutrino flavour isospin (NFIS), that we will use to analyse and visualise collective neutrino oscillations. In section 4.3 we describe an adiabatic MSW-like flavour evolution of dense neutrino gases in the presence of ordinary matter. This type of neutrino oscillation echos the early explorations (e.g. Qian and Fuller, 1995b) where neutrino self-interaction was included as an additional matter effect in the conventional MSW mechanism. In section 4.4 we analyse the stability of bipolar neutrino systems such as supernova neutrinos by utilising the pendulum analogy as well as the simple concept of energy conservation. In section 4.5 we consider the matter effects and try to gain some insights into the qualitative behaviour of neutrino systems as neutrino number densities decrease. We explain why supernova neutrinos do not follow the MSW-like flavour evolution all the way through. In section 4.6 we discuss a collective neutrino oscillation mode which is believed to cause the spectral swap/split, a novel phenomenon revealed in numerical calculations. In section 4.7 we briefly report current understandings of collective neutrino oscillations with full three flavours and/or in realistic supernova environments which are highly inhomogeneous and anisotropic.

#### 4.1. Approximations and numerical results

It is clear that neutrino oscillations in the collective regime must be treated in a way different from that in the pure MSW regime. In the pure MSW regime, the flavour evolution of any single neutrino can be calculated without knowing the flavour states of other neutrinos, as long as the matter densities along the world line (i.e. the matter profile) of this neutrino is given. For a complicated 3D matter profile, the flavour evolution histories of neutrinos propagating along different trajectories can be different even if they are initially in the same flavour state and have the same energy. In the pure MSW regime, this means that the same algorithm for calculating flavour evolution of a single neutrino needs to be run repeatedly for each distinct neutrino beam. In the collective regime, however, because the flavour evolution histories of neutrinos propagating along different trajectories are all coupled, the flavour states of all distinct neutrino beams must be followed simultaneously. While the former problem is ready to be solved given enough computing time, the latter poses such a great numerical challenge that it has not been tackled yet.

Partly because of the complexity of the problem, the supernova models adopted so far to treat neutrino flavour transformation with neutrino self-interaction are all simple and ideal. In these models the supernova environment is spherically symmetric and neutrinos and antineutrinos are emitted isotropically from an infinitely thin neutrino sphere with radius  $R_\nu$ . Neutrinos and antineutrinos are in pure flavour states at the neutrino sphere and encounter only forward-scattering with other particles outside the neutrino sphere. The relativistic effects such as redshift of neutrino energies and gravitational bending of neutrino trajectories are ignored.

In such supernova models nonequivalent neutrino trajectories at radius  $r$  can be distinguished by  $\vartheta$ , the angle between the radial direction and the propagation direction of the neutrino. Equation (17), therefore, becomes

$$[H_{\nu\nu,\vartheta}^{(f)}(r)]_{\alpha\beta} = \frac{\sqrt{2}G_{\text{F}}n_{\nu}^{\text{tot}}(r)}{1 - \cos\vartheta_{\text{max}}(r)} \int_{\cos\vartheta_{\text{max}}(r)}^1 (1 - \cos\vartheta \cos\vartheta') d(\cos\vartheta')$$

$$\begin{aligned} & \times \left[ \sum_{\alpha'} \xi_{\nu_{\alpha'}} \int_0^\infty dE' f_{\nu_{\alpha'}}(E') \langle \nu_\alpha | \psi_{\nu_{\alpha'}}(r) \rangle \langle \psi_{\nu_{\alpha'}}(r) | \nu_\beta \rangle \right. \\ & \left. - \sum_{\alpha'} \xi_{\bar{\nu}_{\alpha'}} \int_0^\infty dE' f_{\bar{\nu}_{\alpha'}}(E') \langle \bar{\nu}_\beta | \psi_{\bar{\nu}_{\alpha'}}(r) \rangle \langle \psi_{\bar{\nu}_{\alpha'}}(r) | \bar{\nu}_\alpha \rangle \right], \end{aligned} \quad (38)$$

where  $\vartheta_{\max}(r) = \arcsin(R_\nu/r)$  is the maximum possible value for  $\vartheta$  at  $r$ ,  $n_\nu^{\text{tot}}(r)$  is the total number density of neutrinos and antineutrinos at  $r$ ,  $\xi_{\nu_\alpha(\bar{\nu}_{\alpha'})}$  and  $f_{\nu_\alpha(\bar{\nu}_{\alpha'})}(E)$  are the fractions of total number flux and normalised energy distributions of neutrinos (antineutrinos) with flavour  $\alpha'$  at the neutrino sphere, and  $|\psi_{\nu_{\alpha'}(\bar{\nu}_{\alpha'})}(r)\rangle$  is the flavour state of a neutrino (antineutrino) initially in flavour  $\alpha'$  and (implicitly) with energy  $E'$  and trajectory angle  $\vartheta'$ .

Even with great simplifications, the “multi-angle approximation” or treatment discussed above is hard to analyse and can be computationally intensive. For these reasons, the early works on the subject adopt what is called the “single-angle approximation”. Under the single-angle approximation neutrino trajectories with different  $\vartheta$  are assumed to be equivalent, and the flavour evolution of neutrinos propagating along a representative trajectory (e.g. the radial trajectory) are computed. The single-angle approximation further simplifies equation (38) and one obtains

$$\begin{aligned} [H_{\nu\nu}^{(f)}(r)]_{\alpha\beta} &= \frac{\mu(r)}{2} \left[ \sum_{\alpha'} \xi_{\nu_{\alpha'}} \int_0^\infty dE' f_{\nu_{\alpha'}}(E') \langle \nu_\alpha | \psi_{\nu_{\alpha'}}(r) \rangle \langle \psi_{\nu_{\alpha'}}(r) | \nu_\beta \rangle, \right. \\ & \left. - \sum_{\alpha'} \xi_{\bar{\nu}_{\alpha'}} \int_0^\infty dE' f_{\bar{\nu}_{\alpha'}}(E') \langle \bar{\nu}_\beta | \psi_{\bar{\nu}_{\alpha'}}(r) \rangle \langle \psi_{\bar{\nu}_{\alpha'}}(r) | \bar{\nu}_\alpha \rangle \right], \end{aligned} \quad (39)$$

where

$$\mu(r) = 2\sqrt{2}G_{\text{F}}n_\nu^{\text{tot}}(r)C(r) \quad (40)$$

is the “effective strength” of neutrino self-interaction at  $r$ . In equation (40)  $C(r)$  is a geometric factor that takes partly into account the angle effects and is

$$C(r) = \frac{\int_{\cos \vartheta_{\max}(r)}^1 (1 - \cos \vartheta') d(\cos \vartheta')}{\int_{\cos \vartheta_{\max}(r)}^1 d(\cos \vartheta')} = \frac{1}{2} \left[ 1 - \sqrt{1 - \left(\frac{R_\nu}{r}\right)^2} \right] \quad (41)$$

if the representative neutrino trajectory is radially oriented. (See [Dasgupta et al, 2008b](#) for a discussion of the single-angle approximation in non-spherical geometry.)

Figure 12 shows the results of the first numerical simulations by [Duan et al \(2006a,b\)](#) of flavour transformation of supernova neutrinos employing the multi-angle treatment. (Also see [Duan et al, 2008a](#) for the movies for the entire simulations.) For comparison the results of the corresponding single-angle calculations are also shown in the same figure. These calculations adopted two-flavour mixing schemes with mass-squared differences  $\delta m^2 \simeq \pm \delta m_{\text{atm}}^2$  and a small mixing angle ( $\theta_\nu = 0.1$ ) representing the unknown value of  $\theta_{13}$ . The mixing occurs between the electronic flavour and the  $\tau'$  flavour, a linear combination of the muon and tau flavours. The matter profile and the neutrino fluxes/spectra used by these calculations correspond to a late-time epoch when r-process nucleosynthesis is supposed to occur.

Figure 12 shows that, in both the normal and inverted neutrino mass hierarchy cases, neutrinos and antineutrinos with various energies propagating along different trajectories can simultaneously experience significant flavour transformation near the PNS. This is clearly different from a standard MSW-flavour-transformation phenomenon. Interestingly, although flavour evolution histories of neutrinos

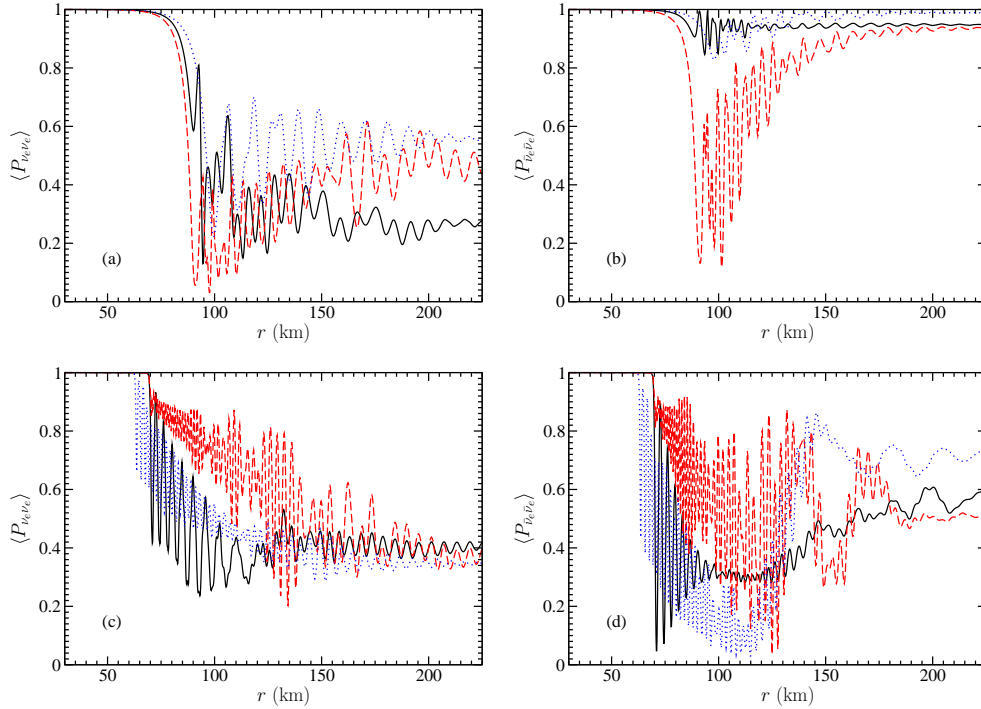


**Figure 12.** Energy-averaged survival probabilities  $\langle P_{\nu\nu} \rangle$  for  $\nu_e$  (left panels) and  $\bar{\nu}_e$  (right panels) as functions of radius  $r$  for the normal (upper panels) and inverted (lower panels) neutrino mass hierarchies, respectively, when neutrino self-interaction is taken into account. The solid and dashed lines give average survival probabilities along the radial and tangential trajectories, respectively, as computed in the multi-angle simulations. The dotted lines give the average survival probabilities computed in the single-angle simulations. Figure adapted from [Duan \*et al\* \(2006a\)](#).

propagating along various trajectories are different in multi-angle calculations, the single-angle calculations seem to share some key qualitative features with their multi-angle counterparts.

Figure 13 reveals an interesting result of collective oscillations of supernova neutrinos which is obtained using the multi-angle treatment. It shows that, when neutrino fluxes have dropped off and collective oscillations end, survival probability  $P_{\nu\nu}$  for the neutrino becomes approximately a step function of neutrino energy  $E_\nu$ . In addition, the directions of these step functions are opposite for the normal and inverted neutrino mass hierarchy cases. The corresponding single-angle calculations yield results that are qualitatively consistent with those employing the multi-angle treatment. The phenomenon seen in figure 13 is called “stepwise spectral swapping” because  $\nu_e$ ’s and  $\nu_{\tau'}$ ’s apparently swap energy spectra at energies below (above) a critical energy  $E_\nu^s$  in a normal (inverted) neutrino mass hierarchy case ([Duan \*et al\*, 2006b](#)). This phenomenon is also known as the “spectral split” since  $E_\nu^s$  “splits the transformed spectrum sharply into parts of almost pure but different flavours” ([Raffelt and Smirnov, 2007b](#)).

Neutrino flavour transformation in supernova with neutrino self-interaction has

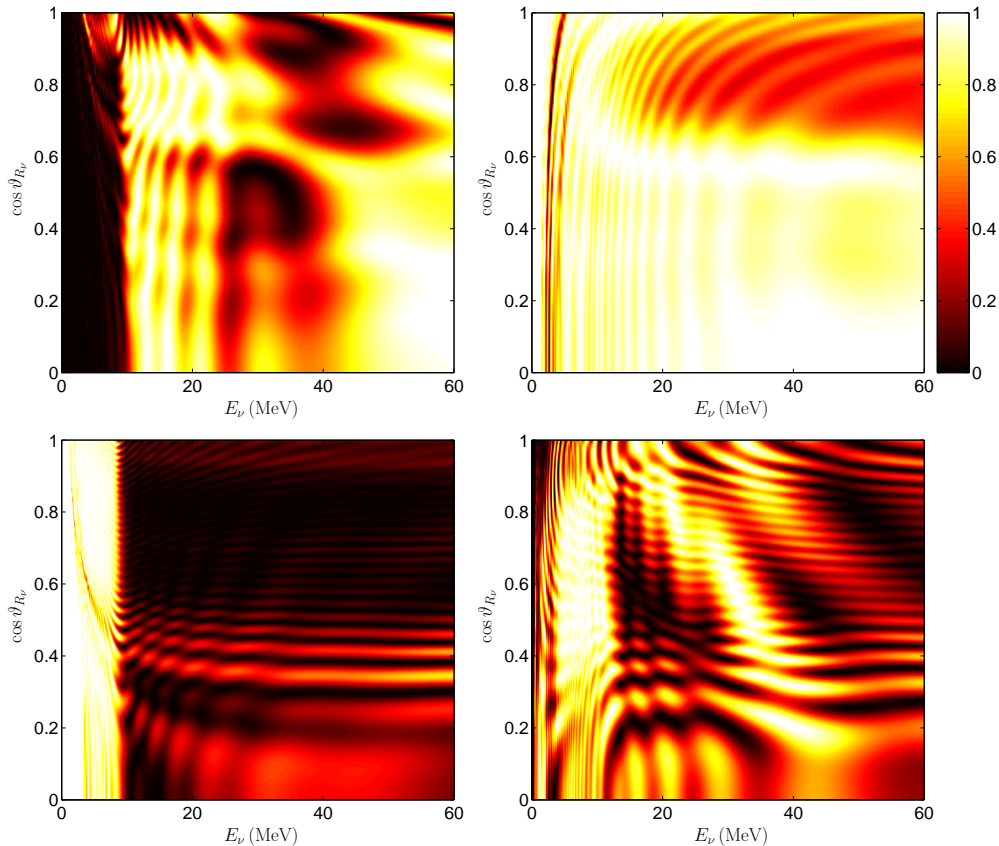


**Figure 13.** Results from the same multi-angle simulations as shown in figure 12. This figure shows survival probabilities  $P_{\nu\nu}$  for neutrinos (left panels) and antineutrinos (right panels) at radius  $r = 225$  km as functions of both neutrino energy  $E_\nu$  and emission angle  $\vartheta_{R_\nu}$ , the angle between the propagation direction of the neutrino and the normal to the neutrino sphere. The upper panels employ a normal neutrino mass hierarchy, and the lower panels employ an inverted neutrino mass hierarchy. The colour scale in the plot denotes the neutrino survival probability with  $P_{\nu\nu} = 1$  being the lightest. Figure adapted from [Duan \*et al\* \(2006a\)](#).

since been studied using both the single-angle and multi-angle treatments. All these calculations confirm that single-angle and multi-angle calculations do share the key common features shown here. Further study by [Duan \*et al\* \(2007b\)](#) showed that the swap/split energy  $E_\nu^s$  decreases significantly with  $\theta_\nu$  in the normal mass hierarchy case and is not sensitive to  $\theta_\nu$  in the inverted mass hierarchy case. Adopting a different matter profile with a thick supernova envelope, [Fogli \*et al\* \(2007\)](#) found no significant flavour transformation of supernova neutrinos in the normal mass hierarchy case and a similar spectral-swap/split phenomenon in the inverted mass hierarchy case.

The single-angle and multi-angle treatments are clearly not equivalent. In fact, the single-angle approximation is not even a self-consistent treatment of the problem. For example, neutrinos propagating along trajectories with different values of  $\vartheta$  travel different distances for any given radius interval. Therefore, if one uses the results from

a single-angle computation and calculates flavour evolution for neutrinos propagating along a trajectory that is different from the representative one, one expects to find results that will contradict the single-angle assumption.

Meanwhile, it is also clear that the single-angle treatment is a much simpler model than the multi-angle one. Although the multi-angle treatment approaches the inhomogeneous and anisotropic nature of the supernova environment in a self-consistent way, it is very difficult to study analytically. Under the single-angle assumption, however, supernova neutrinos are essentially treated as a homogeneous, isotropic neutrino gas with effective neutrino number density

$$n_\nu^{\text{eff}}(r) = n_\nu^{\text{tot}}(r)C(r) \quad (42)$$

that expands with “time”  $r$ . Because the results of the single-angle and multi-angle numerical calculations available so far share many qualitative features, [Duan \*et al\* \(2006b\)](#) conjectured that collective neutrino oscillations in supernovae can be understood, at least qualitatively, by studying similar phenomena in isotropic, homogeneous neutrino gases.

For this reason we shall discuss collective flavour transformation of supernova neutrinos under the single-angle treatment or, equivalently, a homogeneous, isotropic neutrino gas which expands with “time”  $r$ . In the following discussions neutrino number densities must be understood as the effective ones with the geometric factor  $C(r)$  included. [For truly homogeneous, isotropic neutrino gases one has  $C(r) = 1$  and, therefore,  $n_\nu^{\text{eff}}(r) = n_\nu^{\text{tot}}(r)$ .] These analyses shall offer valuable insights into the full-fledged problem of collective neutrino oscillations in realistic supernova environments. In [section 4.7](#) we will briefly summarise the current understandings of collective neutrino flavour transformation in inhomogeneous, anisotropic environments.

#### 4.2. Neutrino flavour isospin

Because  $\hat{H}_{\nu\nu}$  is essentially a sum of matrices of densities for all background neutrinos and antineutrinos, it is convenient to use matrices of densities instead of wavefunctions to describe the flavour states of neutrinos when neutrino self-interaction is important. For a two-flavour mixing scheme, a matrix of density

$$\varrho_{\nu,E} = \frac{1}{2}[n_{\nu,E} + \vec{\sigma} \cdot \vec{P}_{\nu,E}] \quad (43)$$

is equivalent to polarisation vector  $\vec{P}_{\nu,E}$  because the trace of  $\varrho_{\nu,E}$  is not relevant for neutrino oscillations. In [equation \(43\)](#) we have used energy  $E$  to identify a neutrino (or antineutrino) mode in a homogeneous, isotropic neutrino gas, and  $n_{\nu,E}$  is the number density of neutrinos with energy  $E$ . Note that we use “ $\vec{X}$ ” to indicate a vector in flavour space (as compared to vector “ $\mathbf{X}$ ” in coordinate space), and  $\vec{\sigma}$  is such a vector consisting of the three Pauli matrices. Viewing polarisation vectors as “magnetic spins” and neutrino self-interaction as coupling between these spins, [Pastor \*et al\* \(2002\)](#) elucidate the physics mechanism behind synchronisation, a collective neutrino oscillation phenomenon discovered in earlier numerical simulations ([Samuel, 1993](#)). To fully exploit this spin analogy, we will adopt the notation of neutrino flavour isospin (NFIS) defined by [Duan \*et al\* \(2006c\)](#).

For a neutrino (antineutrino) state described by wavefunction  $\psi_{\nu(\bar{\nu}),E}$ , the corresponding NFIS is defined as

$$\vec{s}_\omega = \begin{cases} \psi_{\nu,E}^\dagger \frac{\vec{\sigma}}{2} \psi_{\nu,E} & \text{for neutrino,} \\ (\sigma_y \psi_{\bar{\nu},E})^\dagger \frac{\vec{\sigma}}{2} (\sigma_y \psi_{\bar{\nu},E}) & \text{for antineutrino,} \end{cases} \quad (44)$$

where

$$\omega = \pm \frac{\delta m^2}{2E} \quad (45)$$

with the plus and minus signs for the neutrino and the antineutrino, respectively. The  $\sigma_y$ -transformation of  $\psi_{\bar{\nu},E}$  in equation (44) eliminates the superficial distinction between neutrinos and antineutrinos in the two-flavour mixing scheme. In this notation flavour states of neutrinos and antineutrinos are represented by spins in flavour space with different values of  $\omega$ . In the flavour basis (i.e.  $\psi_{\nu,E} = \langle \nu_\alpha | \psi_{\nu,E} \rangle$ ), the probability for a neutrino to be in  $|\nu_e\rangle$  is given by

$$|\langle \nu_e | \psi_{\nu,E} \rangle|^2 = \frac{1}{2} + \vec{s}_\omega \cdot \vec{e}_z^{(f)}, \quad (46)$$

where  $\vec{e}_z^{(f)}$  is the flavour-basis,  $z$ -direction unit vector in flavour space. Similarly, the probability for an antineutrino to be  $|\bar{\nu}_e\rangle$  is given by

$$|\langle \bar{\nu}_e | \psi_{\bar{\nu},E} \rangle|^2 = \frac{1}{2} - \vec{s}_\omega \cdot \vec{e}_z^{(f)}. \quad (47)$$

NFIS can also be defined from the matrix of density for a neutrino  $\nu$  or antineutrino  $\bar{\nu}$ :

$$\vec{s}_\omega = \begin{cases} \frac{1}{2} \tilde{n}_\omega^{-1} \text{Tr}(\varrho_{\nu,E} \vec{\sigma}) & \text{for neutrino,} \\ \frac{1}{2} \tilde{n}_\omega^{-1} \text{Tr}(\sigma_y \varrho_{\bar{\nu},E} \sigma_y^\dagger \vec{\sigma}) = -\frac{1}{2} \tilde{n}_\omega^{-1} \text{Tr}(\varrho_{\bar{\nu},E}^* \vec{\sigma}) & \text{for antineutrino,} \end{cases} \quad (48)$$

where

$$\tilde{n}_\omega = \sqrt{\sum_{i=x,y,z} [\text{Tr}(\varrho_{\nu(\bar{\nu}),E} \sigma_i)]^2}. \quad (49)$$

Here NFIS  $\vec{s}_\omega$  represents the average flavour of the neutrino (antineutrino) mode  $\omega$ , and  $\tilde{n}_\omega$  is the ‘‘net number density’’ of the neutrino (antineutrino) mode  $\omega$  that is in the flavour state represented by  $\vec{s}_\omega$ . For example, if all neutrinos with energy  $E$  are either in pure  $|\nu_e\rangle$  state or in pure  $|\nu_{\tau'}\rangle$  with number densities  $n_{\nu_e,E}$  and  $n_{\nu_{\tau'},E}$ , respectively, then

$$\vec{s}_\omega = \text{sgn}(n_{\nu_e,E} - n_{\nu_{\tau'},E}) \frac{\vec{e}_z^{(f)}}{2} \quad \text{and} \quad \tilde{n}_\omega = |n_{\nu_e,E} - n_{\nu_{\tau'},E}|.$$

Using  $\tilde{n}_\omega$  we can define the distribution function of NFIS to be

$$\tilde{f}_\omega = \frac{\tilde{n}_\omega(r)}{n_\nu^{\text{eff}}(r)}. \quad (50)$$

We emphasise that, for flavour transformation of supernova neutrinos under the single-angle treatment, all quantities that are proportional to neutrino number densities such as  $n_\nu^{\text{eff}}(r)$  and  $\tilde{n}_\omega(r)$  are computed with the geometric factor  $C(r)$  included. Because we consider only forward scattering between neutrinos and background particles,  $\tilde{f}_\omega$  do not change with  $r$ . We note that  $\tilde{n}_\omega$  is usually less than the neutrino (antineutrino) number density with energy  $|\delta m^2/2\omega|$ . They are equal only if all neutrinos or antineutrinos with this energy are in the same flavour state. As a result, the NFIS distribution function  $\tilde{f}_\omega$  is not normalised to unity but, rather,  $\int_{-\infty}^{\infty} \tilde{f}_\omega d\omega \leq 1$ .

Under the NFIS notation equation (1) becomes

$$\frac{d}{dr} \vec{s}_\omega(r) = \vec{s}_\omega(r) \times \vec{H}_\omega(r) = \vec{s}_\omega(r) \times [\omega \vec{H}_{\text{vac}} + \vec{H}_{\text{matt}}(r) - \mu(r) \langle \vec{s}(r) \rangle], \quad (51)$$

where the misalignment between the “vacuum field”

$$\vec{H}_{\text{vac}} = -\vec{e}_x^{(f)} \sin 2\theta_v + \vec{e}_z^{(f)} \cos 2\theta_v \quad (52)$$

and  $\vec{e}_z^{(f)}$  indicates the mismatch between vacuum mass eigenstates and pure flavour states of neutrinos, the “matter field”

$$\vec{H}_{\text{matt}}(r) = -\sqrt{2}G_{\text{F}}N_{\text{A}}\rho(r)Y_e(r)\vec{e}_z^{(f)} \quad (53)$$

represents the change of refractive indices of neutrinos caused by ordinary matter, and

$$\langle \vec{s}(r) \rangle = \int_{-\infty}^{\infty} d\omega \tilde{f}_\omega \vec{s}_\omega(r) \quad (54)$$

is the average NFIS. Equation (51) shows that NFIS’s are “antiferromagnetically” coupled with each other with strength  $\mu(r) = 2\sqrt{2}G_{\text{F}}n_\nu^{\text{eff}}(r)$ .

In vacuum, NFIS  $\vec{s}_\omega$  precesses around  $\vec{H}_{\text{vac}}$  with angular frequency  $|\omega|$ . When projected to the  $\vec{e}_z^{(f)}$ -axis, this precession motion is interpreted as the oscillation of neutrino flavours [see equations (46) and (47)].

Because of the popular usage of the neutrino polarisation vector, it shall be helpful to discuss the relationship between this notation and the NFIS notation. From equations (43) and (48) it is clear that NFIS’s and neutrino flavour polarisation vectors are connected to each other by simple relations

$$\vec{P}_{\nu,E}(r) = 2n_\nu^{\text{eff}}(r)\tilde{f}_\omega\vec{s}_\omega(r) \quad \text{and} \quad \vec{P}_{\bar{\nu},E}(r) = -2n_{\bar{\nu}}^{\text{eff}}(r)\tilde{f}_\omega\vec{s}_\omega(r). \quad (55)$$

A slightly different definition

$$\vec{P}_\omega(r) \propto \text{sgn}(\omega\delta m^2)\tilde{f}_\omega\vec{s}_\omega(r) \quad (56)$$

is used in some recent literature (e.g. Raffelt and Smirnov, 2007b). With this new definition,  $\vec{P}_\omega(r)$  and  $\vec{s}_\omega(r)$  are related by some constant factor (i.e. independent of  $r$ ) which is positive for a neutrino ( $\omega\delta m^2 > 0$ ) and negative for an antineutrino ( $\omega\delta m^2 < 0$ ). The e.o.m. for  $\vec{P}_\omega(r)$  is

$$\frac{d}{dr}\vec{P}_\omega(r) = [\omega\vec{B} + \lambda(r)\vec{L} + \mu'(r)\vec{D}(r)] \times \vec{P}_\omega(r), \quad (57)$$

where  $\vec{B} = -\vec{H}_{\text{vac}}$ ,  $\lambda(r)\vec{L} = -\vec{H}_{\text{matt}}(r)$ ,  $\mu'(r)$  is different from  $\mu(r)$  by a constant factor depending on the normalisation of  $\vec{P}_\omega(r)$ , and

$$\vec{D}(r) = \int_{-\infty}^{\infty} \text{sgn}(\omega\delta m^2)\vec{P}_\omega(r) d\omega \propto \langle \vec{s}(r) \rangle. \quad (58)$$

We note that the orders of the cross products on the right-hand sides of equations (51) and (57) are different with the former closely imitating the e.o.m. for magnetic spins in magnetic fields.

The notations of the polarisation vector and the NFIS are fully equivalent. However, there is a caveat when the “corotating frame” technique is applied (Duan *et al*, 2006c). In the absence of ordinary matter (i.e.  $\vec{H}_{\text{matt}} = 0$ ) the e.o.m. for the NFIS system is essentially unchanged when observed in a reference frame that rotates about  $\vec{H}_{\text{vac}}$  with a constant angular frequency  $\omega_0$ . The only difference is that the angular precession frequency  $\omega$  of each NFIS  $\vec{s}_\omega(r)$  is shifted by  $-\omega_0$ . This is a powerful technique to analyse collective flavour transformation in neutrino systems. For example, consider a neutrino gas that initially consists of pure  $\nu_e$  and  $\nu_{\tau'}$  with energies  $|\delta m^2/3\omega_0|$  and  $|\delta m^2/\omega_0|$ , respectively. Applying the corotating-frame transformation, one can see that the flavour evolution of this system is similar to that



of the system which initially consists of pure, mono-energetic  $\nu_e$  and  $\bar{\nu}_e$  with energy  $|\delta m^2/\omega_0|$ . We note that a corotating-frame transformation can change the sign of the angular precession frequency  $\omega$  of polarisation vector  $\vec{P}_\omega(r)$ , and the direction of  $\vec{P}_\omega(r)$  must be simultaneously inverted when this occurs. In the NFIS notation, however, the superficial distinction between particles and antiparticles (i.e. the positive and negative frequency modes) is eliminated, and  $\vec{s}_\omega(r)$  is invariant under such a corotating-frame transformation. In some very recent literature (e.g. [Raffelt, 2008](#)) polarisation vectors for antineutrinos are defined in a way similar to NFIS's and have their directions inverted. The caveat discussed above, therefore, disappears under this new definition, and  $\vec{P}_\omega(r)$  and  $\vec{s}_\omega(r)$  are only different by a positive, constant factor that is proportional to  $f_\omega$ .

#### 4.3. Adiabatic MSW-like flavour evolution

Without knowing the results from numerical computations, one may think that the effects of background neutrinos can be treated simply as another potential added to  $V_e(r)$  in the MSW mechanism (e.g. [Qian and Fuller, 1995b](#)). In particular, if both  $\rho(r)$  and  $n_\nu^{\text{eff}}(r)$  vary slowly with  $r$ , one would expect that a neutrino or antineutrino stays in the same matter eigenstate which is essentially a pure flavour state at the neutrino sphere. Of course, a matter eigenstate in this case is an eigenstate of the full Hamiltonian which includes neutrino self-interaction.

Similar to the energy eigenstates of an electron in the presence of a magnetic field, in the NFIS notation the matter eigenstates of neutrinos are represented by spins that are aligned or antialigned with the total effective field  $\vec{H}_\omega(r)$  in flavour space. If supernova neutrinos experience the adiabatic MSW-like flavour evolution described above, one should have

$$\vec{s}_\omega(r) = \frac{\epsilon_\omega}{2} \frac{\vec{H}_\omega(r)}{H_\omega(r)}, \quad (59)$$

or

$$s_{\omega,x}^{(v)}(r) = \frac{\epsilon_\omega}{2H_\omega(r)} [H_{\text{matt},x}^{(v)}(r) - \mu(r)\langle s_x^{(v)}(r) \rangle], \quad (60)$$

$$s_{\omega,y}^{(v)}(r) = -\frac{\epsilon_\omega}{2H_\omega(r)} \mu(r)\langle s_y^{(v)}(r) \rangle, \quad (61)$$

$$s_{\omega,z}^{(v)}(r) = \frac{\epsilon_\omega}{2H_\omega(r)} [\omega + H_{\text{matt},z}^{(v)}(r) - \mu(r)\langle s_z^{(v)}(r) \rangle], \quad (62)$$

where the alignment factor  $\epsilon_\omega$  is constant and equals to +1 (−1) if  $\vec{s}_\omega(R_\nu)$  is aligned (antialigned) with  $\vec{H}_\omega(R_\nu)$ ,  $H_\omega(r) = |\vec{H}_\omega(r)|$ , and  $X_i^{(v)}$  ( $i = x, y, z$ ) stand for the components of vector  $\vec{X}$  in the vacuum mass basis:

$$\vec{e}_x^{(v)} = \vec{e}_x^{(f)} \cos 2\theta_\nu + \vec{e}_z^{(f)} \sin 2\theta_\nu, \quad (63)$$

$$\vec{e}_y^{(v)} = \vec{e}_y^{(f)}, \quad (64)$$

$$\vec{e}_z^{(v)} = \vec{H}_{\text{vac}} = -\vec{e}_x^{(f)} \sin 2\theta_\nu + \vec{e}_z^{(f)} \cos 2\theta_\nu. \quad (65)$$

Averaging equations (60)–(62) over all neutrino modes one obtains

$$\langle s_x^{(v)}(r) \rangle = \frac{1}{2} [H_{\text{matt},x}^{(v)}(r) - \mu(r)\langle s_x^{(v)}(r) \rangle] \int_{-\infty}^{\infty} d\omega \frac{\epsilon_\omega \tilde{f}_\omega}{H_\omega(r)}, \quad (66)$$

$$\langle s_y^{(v)}(r) \rangle = -\frac{1}{2} \mu(r)\langle s_y^{(v)}(r) \rangle \int_{-\infty}^{\infty} d\omega \frac{\epsilon_\omega \tilde{f}_\omega}{H_\omega(r)}, \quad (67)$$

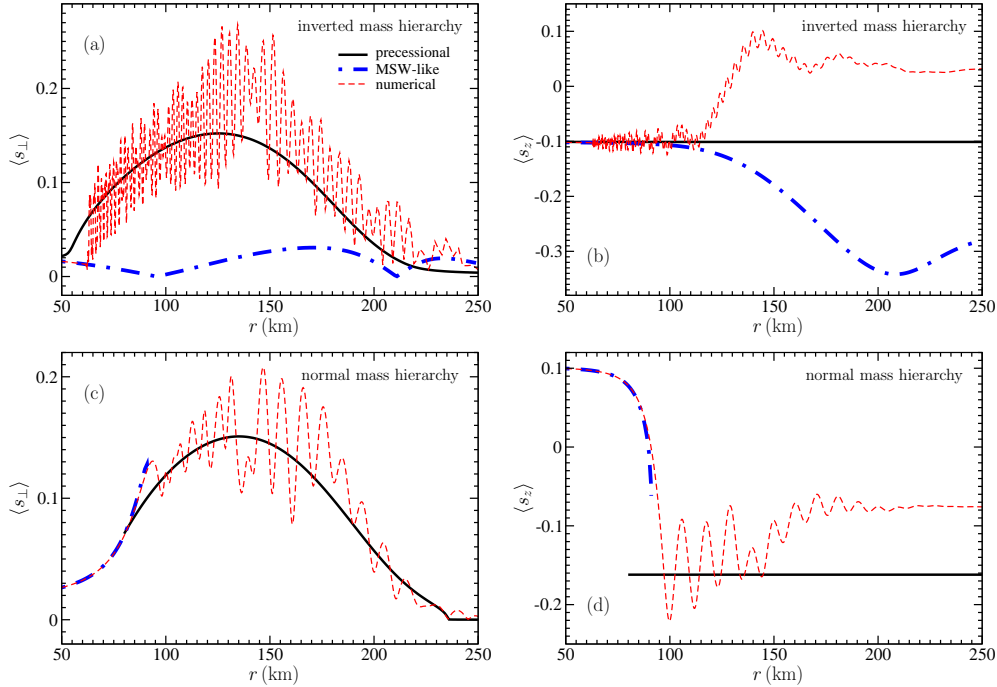


**Figure 14.** Comparison of the results of the single-angle calculations shown in figure 12 with those in the adiabatic MSW-like and adiabatic precession solutions. Figure adapted from Duan *et al* (2007c).

$$\langle s_z^{(v)}(r) \rangle = \frac{1}{2} \int_{-\infty}^{\infty} d\omega \frac{\epsilon_{\omega} \tilde{f}_{\omega}}{H_{\omega}(r)} [\omega + H_{\text{matt},z}^{(v)}(r) - \mu(r) \langle s_z^{(v)}(r) \rangle]. \quad (68)$$

Equations (66) and (67) imply that, if  $\vec{H}_{\text{matt}}(r) \neq 0$ , then  $\langle s_y^{(v)}(r) \rangle = 0$  and, therefore,  $s_{\omega,y}^{(v)}(r) = 0$  for all neutrinos [equation (61)].

If neutrinos follow the adiabatic MSW-like flavour evolution, one can solve equations (66) and (68) for  $\langle s_x^{(v)}(r) \rangle$  and  $\langle s_z^{(v)}(r) \rangle$  and then solve equations (60) and (62) for each individual NFIS. Duan *et al* (2007c) have done exactly that with the same physical settings as those of the single-angle calculations shown in figure 12. The components of the average NFIS  $\langle s_z^{(v)} \rangle$  and  $\langle s_{\perp}^{(v)} \rangle = \sqrt{\langle s_x^{(v)} \rangle^2 + \langle s_y^{(v)} \rangle^2} = |\langle s_x^{(v)} \rangle|$  as functions of  $r$  in this solution are plotted in figure 14. For comparison the results of the corresponding single-angle calculations are also shown in the same figure.

For the inverted mass hierarchy case [figures 14(a,b)] one observes that at  $r \lesssim 63$  km  $\langle s_{\perp}^{(v)}(r) \rangle$  and  $\langle s_z^{(v)}(r) \rangle$  in the single-angle calculation agree very well with the “adiabatic MSW-like solution” which is solved from equations (66) and (68). At  $r \gtrsim 63$  km, however,  $\langle s_{\perp}^{(v)}(r) \rangle$  abruptly jumps out the track of the adiabatic MSW-like flavour evolution. For the normal mass hierarchy case [figures 14(c,d)] the neutrino system follows the adiabatic MSW-like solution to a larger radius. Duan *et al* (2007c) were not able to solve equations (66) and (68) beyond  $r \simeq 91$  km. Figure 14(d) shows that, before the neutrino system deviates from the adiabatic MSW-like flavour evolution, it seems to experience an MSW resonance as  $\langle s_z^{(v)}(r) \rangle$  changes its sign at

$r \simeq 90$  km. [According to equations (46) and (47) the flavour transformation of a neutrino is represented by the changing in the orientation of the correspond NFIS.]

Figure 14 suggests that configuration of the neutrino system becomes unstable just before it departs from the adiabatic MSW-like flavour evolution. This instability is similar to that of a pendulum near its highest position which we will look into next.

#### 4.4. Bipolar systems and flavour pendulum

In simulating neutrino flavour transformation in the early Universe [Kostelecký and Samuel \(1993\)](#) observed an intriguing phenomenon that with an inverted mass hierarchy certain neutrino gases can experience “substantial flavour oscillation even for extremely small mixing angles”. This phenomenon can be partly understood by using the concept of the NFIS energy of a homogeneous, isotropic neutrino gas ([Duan et al, 2006c](#)):

$$\mathcal{E}(t) = - \int_{-\infty}^{\infty} d\omega \tilde{f}_{\omega} \omega \vec{s}_{\omega}(t) \cdot \vec{H}_{\text{vac}} + \frac{\mu(t)}{2} |\langle \vec{s}(t) \rangle|^2, \quad (69)$$

where we have assumed  $\vec{H}_{\text{matt}} = 0$ . Note that the second term on the right-hand side of equation (69) has a positive sign because the NFIS’s are “antiferromagnetically” coupled to each other. Using equation (51) one can show that, if  $n_{\nu}^{\text{eff}}$  and, therefore,  $\mu$  do not vary with time  $t$ ,  $\mathcal{E}$  must also be constant.

As a simple example, we consider a homogeneous and isotropic neutrino gas which initially consists of equal numbers of pure  $\nu_e$  and  $\bar{\nu}_e$  with the same energy  $E_0$ . We assume that  $\vec{H}_{\text{matt}} = 0$  and  $n_{\nu}^{\text{eff}}$  is constant. In the NFIS notation this system is represented by two NFIS’s  $\vec{s}_{\omega_0}(t)$  and  $\vec{s}_{-\omega_0}(t)$  with  $\omega_0 = \delta m^2 / 2E_0$ . At  $t = 0$  NFIS’s  $\vec{s}_{\omega_0}(0)$  and  $\vec{s}_{-\omega_0}(0)$  are aligned and antialigned with  $\vec{e}_z^{(f)}$ , respectively. This is an example of the bipolar system which consists of two groups of NFIS’s approximately opposing each other in direction. According to equation (69) the NFIS energy of such a neutrino gas, up to a constant, is

$$\mathcal{E} = - \frac{\delta m^2}{4E_0} [\vec{s}_{\omega_0}(t) - \vec{s}_{-\omega_0}(t)] \cdot \vec{e}_z^{(v)} + \frac{\sqrt{2}}{2} G_{\text{F}} n_{\nu}^{\text{eff}} [\vec{s}_{\omega_0}(t) \cdot \vec{s}_{-\omega_0}(t)] = \text{const.} \quad (70)$$

When  $n_{\nu}^{\text{eff}}$  is large,  $\mathcal{E}$  is dominated by the coupling energy between the NFIS’s, and, because of energy conservation,  $\vec{s}_{\omega_0}(t)$  and  $\vec{s}_{-\omega_0}(t)$  must remain in a bipolar configuration.

For a normal mass hierarchy ( $\delta m^2 > 0$ ) the initial configuration of our simple bipolar system becomes absolutely stable in the limit  $\theta_{\nu} \rightarrow 0$  (i.e.  $\vec{e}_z^{(f)} \rightarrow \vec{e}_z^{(v)}$ ). This is because in this limit the bipolar system is initially in the lowest energy configuration where both the coupling energy between  $\vec{s}_{\pm\omega_0}$  and  $\vec{H}_{\text{vac}}$  and that between  $\vec{s}_{\omega_0}$  and  $\vec{s}_{-\omega_0}$  are at their minimum values. This is not the case for an inverted mass hierarchy ( $\delta m^2 < 0$ ) with which these two coupling energies are at their maximum and minimum values, respectively. Spontaneous collective neutrino oscillation is, therefore, forbidden to occur in the former case but is allowed in the latter. In fact, if  $\delta m^2 < 0$  and  $G_{\text{F}} n_{\nu}^{\text{eff}} \gg |\delta m^2 / 2E_0|$ , the bipolar configuration of the NFIS’s is energetically allowed to nearly completely flip its direction, and, therefore, both neutrinos and antineutrinos can almost entirely change their flavours.

The flavour dynamics of this bipolar system is probably best illustrated using the pendulum analogy introduced by [Hannestad et al \(2006\)](#). For this bipolar system

equation (51) can be recast in the form

$$\frac{d}{dt}\vec{J}(t) = \vec{q}(t) \times M\vec{g}, \quad (71)$$

$$\vec{J}(t) = M\vec{q}(t) \times \frac{d}{dt}\vec{q}(t) + \sigma\vec{q}(t). \quad (72)$$

Equations (71) and (72) describe the motion of a pendulum with total angular momentum  $\vec{J}(t) = \vec{s}_{\omega_0}(t) + \alpha\vec{s}_{-\omega_0}(t)$ . Here, for more generality, we allow the number densities of antineutrinos and neutrinos to be different with  $\alpha = \tilde{f}_{-\omega_0}/\tilde{f}_{\omega_0}$ . The mass of the pendulum  $M = (1+\alpha)/\mu$  is located at position  $\vec{q}(t) = \vec{Q}(t)/Q$  and it experiences a constant gravity field  $\vec{g} = (Q\omega_0/M)\vec{H}_{\text{vac}}$ , where vector

$$\vec{Q}(t) = \vec{s}_{\omega_0}(t) - \alpha\vec{s}_{-\omega_0}(t) + \frac{1+\alpha}{\mu}\omega_0\vec{H}_{\text{vac}} \quad (73)$$

has a constant length  $Q$ . For  $\alpha \neq 1$  the pendulum moves like a gyroscope because it has a constant, non-vanishing internal spin  $\sigma = \vec{J}(t) \cdot \vec{q}(t)$ .

When neutrino number densities are large, the NFIS's in this example system maintain a bipolar configuration, and  $\vec{q}(t) \simeq 2\vec{s}_{\omega_0}(t) \simeq -2\vec{s}_{-\omega_0}(t)$ . For a normal mass hierarchy ( $\omega_0 > 0$ ),  $\vec{g}$  is in the same direction as that of  $\vec{H}_{\text{vac}}$ . In the limit  $\theta_v \rightarrow 0$ ,  $\vec{q}(t=0) \simeq \vec{H}_{\text{vac}} \simeq \vec{g}/|\vec{g}|$ . In other words, the flavour pendulum is near its lowest position. For an inverted mass hierarchy ( $\omega_0 < 0$ ), however,  $\vec{g}$  is in a direction opposite to that of  $\vec{H}_{\text{vac}}$ . In the limit  $\theta_v \rightarrow 0$ , one has  $\vec{q}(t=0) \simeq -\vec{g}/|\vec{g}|$ , and the flavour pendulum is near its highest position.

The inverted mass hierarchy case with  $\theta_v \ll 1$  is interesting. In this case, if the number densities of neutrinos and antineutrinos are equal, the flavour pendulum will always swing from near the highest position through the lowest position and back to its initial height. During this process bipolar system can experience significant flavour transformation. If the number densities of neutrinos and antineutrinos are different, the pendulum will undergo gyroscopic motion because of its non-vanishing spin, and it will not pass through the lowest position. In particular, the pendulum will remain at its highest position like a ‘‘sleeping top’’ if (e.g. Scarborough, 1958)

$$\frac{\sigma^2}{4M^2g} \geq 1. \quad (74)$$

For the simple bipolar neutrino system shown above, this is equivalent to the condition that (Duan *et al*, 2007a; Hannestad *et al*, 2006)

$$n_\nu^{\text{eff}} \geq \frac{\sqrt{2}}{2} \frac{1+\alpha}{(1-\sqrt{\alpha})^2} \frac{|\delta m^2|}{G_{\text{F}}E_0}. \quad (75)$$

This condition can be viewed as the division between the so-called ‘‘synchronised regime’’ and the ‘‘bipolar regime’’ for the following reasons.

According to equation (51) each individual NFIS  $\vec{s}_\omega(t)$  tends to precess about  $\vec{H}_{\text{vac}}$  with its angular frequency  $\omega$ . At the same time, the coupling among NFIS's tend to make them move collectively. If the latter tendency dominates, all the NFIS's are locked into one block spin with angular precession frequency

$$\omega_{\text{sync}} = \int_{-\infty}^{\infty} d\omega' \omega' \tilde{f}_{\omega'} \frac{\vec{s}_{\omega'} \cdot \langle \vec{s} \rangle}{|\langle \vec{s} \rangle|^2}. \quad (76)$$

This is the synchronised neutrino flavour transformation explained by [Pastor \*et al\* \(2002\)](#). A necessary condition of synchronisation is that each NFIS precesses about the block spin much faster than does the block spin about  $\vec{H}_{\text{vac}}$ , i.e.

$$\mu|\langle\vec{s}\rangle| \gtrsim |\omega_{\text{sync}}|. \quad (77)$$

[Duan \*et al\* \(2006c\)](#) pointed that a bipolar system can experience synchronised or bipolar (pendulum-like) oscillations depending on whether condition (77) is satisfied. For the simple bipolar system discussed above, the estimates given by equations (75) and (77) for  $n_\nu^{\text{eff}}$  at the boundary between the synchronised and bipolar regimes are different only by a constant factor.

#### 4.5. Transition to bipolar oscillations

[Pastor and Raffelt \(2002\)](#) proposed that supernova neutrinos could experience synchronised flavour transformation when neutrino fluxes are very large. Using equation (77) [Duan \*et al\* \(2006c\)](#) determined the synchronised and bipolar regimes in the supernova environment. The notion of the synchronised regime has since then been widely adopted. However, figure 14 shows that neutrinos actually experience the MSW-like flavour evolution instead of the synchronised flavour transformation in the so-called synchronised regime when  $\vec{H}_{\text{matt}} \neq 0$ . In addition, in the normal mass hierarchy case supernova neutrinos follow the MSW-like flavour evolution well beyond the synchronised regime as determined in the inverted mass hierarchy case (figure 14).

[Duan \*et al\* \(2007c\)](#) proposed that flavour transformation of supernova neutrinos in the collective regime, i.e. neutrino self-interaction is not negligible, can be explained as the combination of two adiabatic solutions, i.e. the adiabatic MSW-like solution discussed in section 4.3 and the adiabatic precession solution to be described in section 4.6. The flavour pendulum model discussed in section 4.4 offers great insights into the question why neutrinos deviate from the adiabatic MSW-like flavour evolution in supernovae. We shall elaborate on this idea in more detail.

We note that at the neutrino sphere the most abundant neutrino species are  $\nu_e$  and  $\bar{\nu}_e$ , which is similar to the simplistic bipolar system represented by the flavour pendulum model. In addition, as pointed out by [Duan \*et al\* \(2006c\)](#), the effects of ordinary matter can be “ignored” for collective neutrino oscillations even if the density of ordinary matter is large (but still low enough to be transparent to neutrinos). The idea of ignoring ordinary matter is at the core of the collective flavour transformation of supernova neutrinos and we shall discuss it first.

According to equation (51), all NFIS’s tend precess to about the matter field  $\vec{H}_{\text{matt}}$  with the same frequency and, therefore,  $\vec{H}_{\text{matt}}$  does not break the collectiveness of neutrino oscillations as  $\vec{H}_{\text{vac}}$  does. In fact, the matter field “disappears” in the reference frame that rotates about  $\vec{H}_{\text{matt}}$  with angular frequency  $|\vec{H}_{\text{matt}}|$ . This is similar to the situation where the gravity field “vanishes” in a freely-falling reference frame. In this corotating frame, however,  $\vec{H}_{\text{vac}}$  is not stationary but rotates about  $-\vec{H}_{\text{matt}}$  with angular frequency  $|\vec{H}_{\text{matt}}|$ . If the matter density is large,  $\vec{H}_{\text{vac}}^\perp$ , the component of  $\vec{H}_{\text{vac}}$  that is perpendicular to  $\vec{H}_{\text{matt}}$ , rotates very fast about  $\vec{H}_{\text{matt}}$ . As a result, its effects on NFIS’s average to zero if the NFIS’s participate in some collective motion with a time scale much longer than  $2\pi/|\vec{H}_{\text{matt}}|$ . In other words, when the matter density is large, one can ignore the effects of ordinary matter for collective neutrino oscillations by adopting a small effective mixing angle and an effective mass-squared difference  $\delta m_{\text{eff}}^2 = \delta m^2 \cos 2\theta_\nu$ . [Hannestad \*et al\* \(2006\)](#) analysed the effects

of ordinary matter on the flavour pendulum and confirmed that matter density had little effect on the motion of the pendulum except for a logarithmic dependence of the period of this motion on the matter density.

Let us now consider the inverted mass hierarchy case with  $\theta_v \ll 1$ . We can estimate when bipolar oscillations may start using the analogy of the flavour pendulum. Near the neutrino sphere the effective total neutrino number density  $n_\nu^{\text{eff}}(r)$  is large, and the mass of the pendulum  $M \propto (n_\nu^{\text{eff}})^{-1}$  is small. As a result, the pendulum with nonzero spin  $\sigma \simeq (1 - \alpha)/2$  is able to “defy” gravity and stays at its highest position. In other words, no significant bipolar oscillation can occur and supernova neutrinos follow the adiabatic MSW-like flavour evolution in which both neutrinos and antineutrinos essentially remain in their original flavours. As neutrino number densities decrease with  $r$  the mass of the flavour pendulum increases. Eventually, the flavour pendulum becomes so heavy that its highest position is no longer stable [see equation (74)]. When this occurs, supernova neutrinos will break away from the MSW-like flavour evolution and experience the bipolar oscillation. As mentioned earlier, unlike in the MSW-like flavour evolution, the presence of ordinary matter will not affect the bipolar oscillation once it starts.

Bipolar neutrino oscillations are represented by the gyroscopic motion of the flavour pendulum which is a combination of nutation and precession. The nutation of the flavour pendulum signifies simultaneous oscillations of  $s_{\omega,z}$ , the  $z$  components of the NFIS’s, or the oscillations neutrino survival probabilities (see figure 12). Here we do not distinguish between the vacuum mass basis and the flavour basis because the effective mixing angle is small. The precession of the flavour pendulum stands for the simultaneous precession of all NFIS’s about the  $z$  axis in flavour space. From the above discussion it is clear that in the inverted mass hierarchy case bipolar oscillations are insensitive to the exact value of  $\theta_v$ . This explains why Duan *et al* (2007b) obtained similar results for different inverted mass hierarchy schemes even when  $\theta_v$  differ by several orders of magnitude. It is also obvious that bipolar oscillations are not sensitive to large matter densities in inverted mass hierarchy cases as confirmed by Fogli *et al* (2007).

For the normal mass hierarchy case, the flavour pendulum is initially near its lowest position where it is stable even when  $n_\nu^{\text{eff}}(r)$  decreases. As a result, in the single-angle calculations presented in figure 12, supernova neutrinos follow the adiabatic MSW-like evolution until they experience significant flavour transformation at  $r \simeq 90$  km because of low matter density. This flavour transformation is similar to the resonance in the conventional MSW mechanism and is represented by flipping of the orientation of the NFIS’s or raising of the flavour pendulum. As in the inverted mass hierarchy case, the flavour pendulum will undergo gyroscopic motion after the pendulum is raised and supernova neutrinos will, therefore, experience bipolar oscillations. But unlike the inverted hierarchy case, the initiation of bipolar oscillations depends upon the existence/efficacy of MSW-like resonances. So for the normal hierarchy collective neutrino flavour transformation is inevitably sensitive to the value of  $\theta_v$  and matter densities, an expectation confirmed by Duan *et al* (2007b) and Fogli *et al* (2007), respectively.

#### 4.6. Adiabatic precession solution

Comparing figures 12(c,d) and 14(b) one notices that, although individual NFIS’s can oscillate with significant amplitudes in the  $z$  direction,  $\langle s_z(r) \rangle$  roughly stays constant

at  $r \lesssim 100$  km. This is because, as pointed out by [Hannestad \*et al\* \(2006\)](#), neutrino lepton number

$$L = 2 \int_{-\infty}^{\infty} d\omega \tilde{f}_\omega \vec{s}_\omega(r) \cdot \vec{H}_{\text{vac}} = 2 \langle s_z^{(\nu)}(r) \rangle \quad (78)$$

is constant if the matter field can be “ignored”. This conservation law arises because, when the matter field is absent, there is only one external field  $\vec{H}_{\text{vac}}$  in the NFIS system, and the e.o.m. for the NFIS’s are invariant with a simultaneous rotation of all NFIS’s about  $\vec{H}_{\text{vac}}$ . However, this symmetry about  $\vec{H}_{\text{vac}}$  is usually broken because most configurations of NFIS systems are not invariant with rotation about  $\vec{H}_{\text{vac}}$ . As a result the NFIS’s tend to rotate about  $\vec{H}_{\text{vac}}$  collectively in order to restore the symmetry dynamically.

The collective mode of neutrino oscillations discussed above corresponds to the precession motion of a flavour pendulum. If a pendulum undergoes pure precession without wobbling, its motion is symmetric about the  $z$  axis although its configuration at any instant is not. One can imagine that such a pendulum will slowly fall but remain in pure precession if its weight and spin are changed infinitely slowly. [Duan \*et al\* \(2007a\)](#) studied the flavour evolution of the simple bipolar system discussed in section 4.4 assuming that the flavour pendulum stays in pure precession as  $n_\nu^{\text{eff}}(r)$  decreases. They found qualitative agreement between this simple analysis and the numerical simulations of flavour evolution of supernova neutrinos.

Neutrino gases in the pure collective precession mode satisfy two conditions, namely, the pure precession ansatz and the adiabatic ansatz ([Duan \*et al\*, 2008d](#)). The precession ansatz is that at any instant all NFIS’s precess about  $\vec{H}_{\text{vac}}$  with the same angular frequency  $\omega_{\text{pr}}(n_\nu^{\text{eff}})$  which varies with  $n_\nu^{\text{eff}}$ , or

$$\frac{d}{dr} \vec{s}_\omega(r) = \vec{s}_\omega(r) \times \omega_{\text{pr}}(n_\nu^{\text{eff}}) \vec{H}_{\text{vac}}. \quad (79)$$

From equation (79) and the e.o.m. for NFIS’s [equation (51)] one concludes that each NFIS  $\vec{s}_\omega(r)$  must be either aligned or antialigned with

$$\vec{H}_\omega(r) = \vec{H}_\omega(r) - \omega_{\text{pr}}(n_\nu^{\text{eff}}) \vec{H}_{\text{vac}} = [\omega - \omega_{\text{pr}}(n_\nu^{\text{eff}})] \vec{H}_{\text{vac}} - \mu(n_\nu^{\text{eff}}) \langle \vec{s}(r) \rangle. \quad (80)$$

In other words, condition

$$\vec{s}_\omega(r) = \frac{\epsilon_\omega}{2} \frac{\vec{H}_\omega(r)}{|\vec{H}_\omega(r)|} \quad (81)$$

holds, where  $\epsilon_\omega = +1$  or  $-1$  if  $\vec{s}_\omega(r)$  is aligned or antialigned with  $\vec{H}_\omega(r)$ . Note that we have ignored  $\vec{H}_{\text{matt}}$  in discussion of collective neutrino oscillations.

If  $n_\nu^{\text{eff}}(r)$  varies slowly with  $r$ , the NFIS system transits from state to state all of which satisfy the precession ansatz. The adiabatic ansatz is that  $\epsilon_\omega$  stays constant during these transitions:

$$\frac{d}{dr} \epsilon_\omega = 0. \quad (82)$$

[Duan \*et al\* \(2006b\)](#) showed that the spectral-swap/split phenomenon (figure 13) can arise as a result of collective precession of NFIS’s using the following simple argument. If neutrinos are in the pure collective precession mode, each NFIS  $\vec{s}_\omega(r)$

must stay aligned or antialigned with  $\vec{H}_\omega(r)$  depending on the value of  $\epsilon_\omega$ . This is true even when  $n_\nu^{\text{eff}} \rightarrow 0$ . In this limit one simply have

$$\vec{s}_\omega|_{n_\nu^{\text{eff}} \rightarrow 0} = \frac{\epsilon_\omega}{2} \text{sgn}(\omega - \omega_{\text{pr}}^0) \vec{e}_z^{(\nu)}, \quad (83)$$

where  $\omega_{\text{pr}}^0 = \omega_{\text{pr}}(n_\nu^{\text{eff}} = 0)$ . Equation (83) implies that the NFIS orientation  $\vec{s}_\omega|_{n_\nu^{\text{eff}} \rightarrow 0}$  as a function of  $\omega$  flips direction at  $\omega_{\text{pr}}^0$ . For  $\theta_\nu \ll 1$  this means that the neutrino survival probability as a function of neutrino energy jumps from 0 to 1 or vice versa at energy  $|E_\nu^{\text{s}}|$ , where

$$E_\nu^{\text{s}} = \frac{\delta m^2}{2\omega_{\text{pr}}^0}. \quad (84)$$

The swapping point is located in the neutrino (antineutrino) sector if  $E_\nu^{\text{s}} > 0$  ( $E_\nu^{\text{s}} < 0$ ). For  $E_\nu^{\text{s}} > 0$  the whole energy spectra of antineutrinos stay the same or get swapped depending on whether the neutrino mass hierarchy is normal or inverted. Raffelt and Smirnov (2007b) pointed out that the value of  $\omega_{\text{pr}}^0$  or  $E_\nu^{\text{s}}$  can be determined using equation (83) and the conservation of lepton number  $L$  defined in equation (78):

$$L = \int_{-\infty}^{\infty} d\omega \tilde{f}_\omega \epsilon_\omega \text{sgn}(\omega - \omega_{\text{pr}}^0). \quad (85)$$

Raffelt and Smirnov (2007b) showed that, for homogeneous, isotropic neutrino gases or supernova neutrinos under the single-angle approximation, the pure collective precession mode of neutrino oscillations with any given  $n_\nu^{\text{eff}}$  can be solved from a small set of nonlinear equations. One notes that  $\vec{H}_\omega(r)$  is the total effective field for  $\vec{s}_\omega(r)$  in the frame that rotates about  $\vec{H}_{\text{vac}}$  with angular frequency  $\omega_{\text{pr}}(n_\nu^{\text{eff}})$ . Because a NFIS is only stationary when it is either aligned or antialigned with its total effective field, the precession ansatz is equivalent to the assumption that it is possible to find a corotating frame in which all NFIS's are stationary. In this corotating frame equation (81) is equivalent to

$$s_{\omega, \tilde{x}} = -\frac{\epsilon_\omega}{2} \frac{\mu \langle s_{\tilde{x}} \rangle}{\sqrt{(\omega - \omega_{\text{pr}} - \mu \langle s_z \rangle)^2 + (\mu \langle s_{\tilde{x}} \rangle)^2}}, \quad (86)$$

$$s_{\omega, z} = \frac{\epsilon_\omega}{2} \frac{\omega - \omega_{\text{pr}} - \mu \langle s_z \rangle}{\sqrt{(\omega - \omega_{\text{pr}} - \mu \langle s_z \rangle)^2 + (\mu \langle s_{\tilde{x}} \rangle)^2}}, \quad (87)$$

where  $s_{\omega, \tilde{x}}$  is the projection of  $\vec{s}_\omega$  on  $\vec{e}_{\tilde{x}}$ . Here we define  $\vec{e}_{\tilde{x}}$  to be the unit vector in the same direction of  $\langle \vec{s}_\perp \rangle$ , the vector component of  $\langle \vec{s} \rangle$  which is perpendicular to  $\vec{e}_z^{(\nu)}$ . Multiplying equations (86) and (87) with  $\tilde{f}_\omega$  and integrating them over  $\omega$  one obtains

$$1 = -\frac{1}{2} \int_{-\infty}^{\infty} d\omega \frac{\epsilon_\omega \tilde{f}_\omega}{\sqrt{[(\omega - \omega_{\text{pr}})/\mu - \langle s_z \rangle]^2 + \langle s_{\tilde{x}} \rangle^2}}, \quad (88)$$

$$\omega_{\text{pr}} = -\frac{1}{2} \int_{-\infty}^{\infty} d\omega \frac{\epsilon_\omega \tilde{f}_\omega \omega}{\sqrt{[(\omega - \omega_{\text{pr}})/\mu - \langle s_z \rangle]^2 + \langle s_{\tilde{x}} \rangle^2}}. \quad (89)$$

Note that in equations (88) and (89) the minus signs arise because of the antiferromagnetic coupling between NFIS's. Given  $(L, n_\nu^{\text{eff}}, \epsilon_\omega)$  one can solve equations (78), (88) and (89) for  $(\omega_{\text{pr}}, \langle s_{\tilde{x}} \rangle, \langle s_z \rangle)$ . One can then solve equations (86) and (87) for each individual NFIS.

Duan *et al* (2007c) solved the adiabatic, precession solution from equations (78) and (86)–(89) that corresponds to the single-angle calculations presented earlier.



The results are plotted in figure 14 together with the results from single-angle calculations and the corresponding adiabatic, MSW-like solutions. One observes that  $\langle s_{\perp}(r) \rangle = |\langle s_{\bar{x}}(r) \rangle|$  obtained in single-angle calculations oscillate around the adiabatic precession solution after neutrinos stop following the adiabatic MSW-like flavour evolution. The values of  $\langle s_z(r) \rangle$  are approximately constant when the collection precession mode first sets in but then changes as the densities of both ordinary matter and neutrinos continue to decrease with  $r$  and conventional MSW flavour conversion starts to intervene.

#### 4.7. Collective neutrino oscillations in realistic supernova environments

We have so far summarised our understanding of collective neutrino oscillations under the assumptions that both the two-flavour neutrino mixing scheme and the single-angle treatment of a spherical supernova model are valid. The results obtained using these assumptions shed light on, and form the basis of, our understanding of three-flavour, collective neutrino oscillations in realistic supernova environments. Here we briefly report the progresses made in these directions.

Duan *et al* (2008b) carried out the first single-angle calculations which take into account neutrino self-interaction and use the full three-flavour neutrino mixing. These calculations are targeted at a very early epoch of an O-Ne-Mg core-collapse supernova when the fast deleptonization of the PNS leads to an intense  $\nu_e$  burst. These calculations show that the neutrino energy spectra emerged from the supernova surface can also contain step-like features as in two-flavour calculations. The results of these calculations also suggest that, like in the conventional MSW flavour transformation, collective neutrino oscillations in the full three-flavour mixing scheme can be factorised into two two-flavour mixing scenarios that occur in sequence.

To generalise the spin-precession analogy to three flavour oscillations, Dasgupta and Dighe (2008) defined eight-dimensional Bloch vector  $\vec{P}_{\omega}$ , the three-flavour version of the polarisation vector, as

$$\varrho_{\omega} = \frac{n_{\nu}^{\text{eff}}}{3} + \frac{1}{2} \vec{P}_{\omega} \cdot \vec{\Lambda}, \quad (90)$$

where  $\Lambda_i$  ( $i = 1, 2, \dots, 8$ ) are the Gell-Mann matrices. One can define the cross product of eight-dimensional vectors by replacing the structure constant  $\epsilon_{ijk}$  of the SU(2) group with the structure constant  $f_{ijk}$  of SU(3) (Kim *et al*, 1988). The e.o.m. for  $\vec{P}_{\omega}$  can then be written in a form similar to equation (57). With Bloch vectors, three-flavour collective neutrino oscillations can be visualised by the “ $\vec{e}_3$ - $\vec{e}_8$ ” diagram, where  $\vec{e}_i$  ( $i = 1, 2, \dots, 8$ ) are the unit basis vectors for the eight-dimensional flavour space. Using the concept of Bloch vectors and a simplified supernova model Dasgupta *et al* (2008c) showed that the step-like features in the energy spectra of supernova neutrinos in Duan *et al* (2008b) can indeed be understood as two spectral swaps/splits each of which corresponds to the conservation of a neutrino lepton number.

Independently, Duan *et al* (2008d) attacked the problem of three-flavour, collective neutrino oscillations using a different approach. Using the correspondence between the operations for NFIS’s and flavour matrices:

$$\vec{s}_{\omega} \times \vec{s}_{\omega'} \sim [\varrho_{\omega}, \varrho_{\omega'}] \quad \text{and} \quad \vec{s}_{\omega} \cdot \vec{s}_{\omega'} \sim \text{Tr}(\varrho_{\omega} \varrho_{\omega'}), \quad (91)$$

one can translate the analyses for two-flavour neutrino mixing from the spin representation to matrix representation. In this translation a corotating frame is equivalent to a unitary transformation. Similarly, the statement that a NFIS  $\vec{s}_{\omega}$  is

stationary in such a corotating frame means that  $\varrho_\omega$  commutes with its Hamiltonian after an appropriate unitary transformation. Expressing the precession ansatz [equation (79)] and the adiabatic ansatz [equation (82)] in terms of flavour matrices and generalising them to the three-flavour mixing scheme, Duan *et al* (2008d) showed that the e.o.m. for  $\varrho_\omega$  in the three-flavour scheme are invariant under independent rotations of the whole system about  $\Lambda_3$  and  $\Lambda_8$  when the matter field is absent. Two collective precession modes of neutrino oscillations can arise because of these symmetries which would naturally lead to spectral swaps/splits as in three-flavour mixing scenarios.

While all of the above analyses on collective neutrino oscillations are based on the homogeneity and isotropy of the neutrino gas or the validity of the single-angle approximation of supernova neutrinos, a real supernova environment is clearly inhomogeneous and anisotropic. Some of the conclusions that are correct for homogeneous, isotropic neutrino gases may not be so for inhomogeneous, anisotropic ones. For example, Esteban-Pretel *et al* (2008a) recently showed that very dense ordinary matter can play a bigger role in suppressing collective neutrino oscillations in anisotropic environments than in isotropic environments.

Raffelt and Sigl (2007) studied some simple anisotropic neutrino gases initially consisting of neutrinos and antineutrinos with equal numbers. They found that collective oscillations in such systems quickly break down and flavour equipartition is always achieved. We note that such a system correspond to a flavour pendulums with no internal spin which does not undergo precession at all. This study, therefore, suggests that bipolar neutrino oscillations that correspond to the nutation motion of the flavour pendulum are not collective in anisotropic environments. However, the collective neutrino oscillation mode that corresponds to the precession motion of the flavour pendulum arises because of a symmetry in the equations that govern flavour evolution of neutrinos. This symmetry also exists in inhomogeneous, anisotropic neutrino gases (Duan *et al*, 2008c). Protected by this symmetry, the collective precession mode of neutrino flavour transformation may not break down even in inhomogeneous, anisotropic environments. Indeed, Esteban-Pretel *et al* (2007) showed that single-angle-like collective neutrino oscillations appear as the neutrino-antineutrino symmetry is dropped which permits the precession motion of the flavour pendulum.

Using the symmetry of the equations that govern neutrino flavour evolution Duan *et al* (2008c) prescribed the adiabatic, precessional flavour evolution in inhomogeneous, anisotropic neutrino gases, which is similar to the simpler cases with homogeneous and isotropic neutrino gases. The key idea is that, assuming all NFIS's to precess collectively about  $\vec{H}_{\text{vac}}$ , at any *space-time point* (instead of any instant in homogeneous, isotropic cases) one can find a corotating frame in which all the NFIS's at this point are stationary. Such a collective neutrino oscillation mode is described by a wave-like solution. As neutrinos travel from one “wavefront” to another, the corresponding NFIS's rotate about  $\vec{H}_{\text{vac}}$  with a common angle which is equal to the phase difference between the two “wavefronts” of the solution.

## 5. Summary and outlook

While the neutrino telescopes around the globe are waiting for the neutrino shower from the next Galactic supernova, our rapidly-growing knowledge of neutrino flavour transformation in supernovae suggests that these cosmic neutrinos will reveal much valuable information about the supernova as well as about themselves. Through these

neutrinos the dynamical features of the supernova such as shocks and turbulence may be observed and analysed. Undetermined fundamental properties of the neutrino such as its mass hierarchy may be disclosed through the swapped/split neutrino energy spectra due to neutrino self-interaction. However, much still need to be learned about this subject.

For example, collective neutrino oscillations in highly inhomogeneous, anisotropic environments are so far not well understood. Most of our understanding of collective neutrino oscillations is based on the single-angle approximation which ignores the anisotropic nature of the supernova environment. Meanwhile, direct numerical simulation of neutrino oscillations with neutrino self-interaction in such environments (using 2D and/or 3D matter profiles) remains to be done. The subject of turbulence in supernova and its impact is also uncertain. One of the imminent tasks is to combine the effect of the dynamic matter profile and that of neutrino self-interaction, which has been studied largely in parallel so far. The matter contribution is important near the region where  $G_F \rho(r) \sim \delta m^2/(2E)$  and collective neutrino oscillations can occur if  $G_F n_\nu(r) \gtrsim \delta m^2/(2E)$ . If the two regions are well separated, one can conduct two calculations in series with the results from the computation of collective oscillations as inputs to that on the MSW effect. This is the approximation made by Chakraborty *et al* (2008); Gava *et al* (2009); Kneller *et al* (2008); Lunardini *et al* (2008). In the case where the two regions overlap with each other, in principle one should carry out a comprehensive calculation with both effects included which could be a time-consuming task.

In summary, we have reviewed the field of neutrino oscillations in supernovae focusing upon the recent discoveries of the dynamism of the pure-MSW effect and the emergence of neutrino self-interactions near the neutrino sphere. We have attempted to give those readers interested in pursuing research in this area sufficient detail that he or she can now begin to digest the ever-growing literature on the subject and, at the same time, give the casual observer a overarching understanding of these two phenomena. But perhaps the most general summary we can make is that the evolution of this field over the past few years has been both fruitful and frenetic and we fully expect that this trend will continue for some time yet.

## Acknowledgments

The authors are very grateful to the editor for giving us the opportunity to write this review and to G M Fuller, J Gava, R Humphreys, G McLaughlin, A Mirizzi, Y-Z Qian, and C Volpe for the discussions during the drafting process. This work was supported in part by US DOE grants DE-FG02-00ER41132 at INT and DE-FG02-87ER40328 at UMN, and by “Non standard neutrino properties and their impact in astrophysics and cosmology”, Project No. ANR-05-JCJC-0023 at IPN Orsay.

## References

- Ahmad Q R *et al* (SNO) 2002 *Phys. Rev. Lett.* **89** 011301  
 Ahrens J *et al* (AMANDA) 2002 *Astropart. Phys.* **16** 345 (*Preprint* arXiv:astro-ph/0105460)  
 Alekseev E N, Alekseeva L N, Volchenko V I and Krivosheina I V 1987 *Pis'ma Zh. Eksp. Teor. Fiz.* **45** 461 (*JETP Lett.* **45** 589)  
 Amsler C *et al* (Particle Data Group) 2008 *Phys. Lett. B* **667** 1

- Arcones A, Janka H-T and Scheck L 2007 *Astron. Astrophys.* **467** 1227 (*Preprint* arXiv:astro-ph/0612582)
- Arnett W D 1982 *Astrophys. J. Lett.* **263** L55
- Aschenbach B, Egger R and Trumper J 1995 *Nature* **373** 587
- Baade W and Zwicky F 1934 *Proc. Natl. Acad. Sci. USA* **20** 259
- Bahcall J N and Sears R L 1972 *Ann. Rev. Astron. Astrophys.* **10** 25
- Balantekin A B, Fetter J M and Loreti F N 1996 *Phys. Rev. D* **54** 3941 (*Preprint* arXiv:astro-ph/9604061)
- Balantekin A B and Fuller G M 2003 *J. Phys. G* **29** 2513 (*Preprint* arXiv:astro-ph/0309519)
- Balantekin A B, Gava J and Volpe C 2008 *Phys. Lett. B* **662** 396 (*Preprint* arXiv:0710.3112)
- Balantekin A B and Pehlivan Y 2007 *J. Phys. G* **34** 47 (*Preprint* arXiv:astro-ph/0607527)
- Balantekin A B and Yüksel H 2005 *New J. Phys.* **7** 51 (*Preprint* arXiv:astro-ph/0411159)
- Beacom J F, Farr W M and Vogel P 2002 *Phys. Rev. D* **66** 033001 (*Preprint* arXiv:hep-ph/0205220)
- Bell N F, Rawlinson A A and Sawyer R F 2003 *Phys. Lett. B* **573** 86 (*Preprint* arXiv:hep-ph/0304082)
- Benatti F and Floreanini R 2005 *Phys. Rev. D* **71** 013003 (*Preprint* arXiv:hep-ph/0412311)
- Bethe H A and Wilson J R 1985 *Astrophys. J.* **295** 14
- Beun J, McLaughlin G C, Surman R and Hix W R 2006 *Phys. Rev. D* **73** 093007 (*Preprint* arXiv:hep-ph/0602012)
- Bionta R M *et al* 1987 *Phys. Rev. Lett.* **58** 1494
- Blondin J M 2005 *J. Phys. Conf. Ser.* **16** 370
- Blondin J M and Mezzacappa A 2006 *Astrophys. J.* **642** 401 (*Preprint* arXiv:astro-ph/0507181)
- Blondin J M and Mezzacappa A 2007 *Nature* **445** 58 (*Preprint* arXiv:astro-ph/0611680)
- Blondin J M, Mezzacappa A and DeMarino C 2003 *Astrophys. J.* **584** 971 (*Preprint* arXiv:astro-ph/0210634)
- Blondin J M and Shaw S 2007 *Astrophys. J.* **656** 366 (*Preprint* arXiv:astro-ph/0611698)
- Brown G E, Bethe H A and Baym G 1982 *Nucl. Phys. A* **375** 481
- Buras R, Rampp M, Janka H-T and Kifonidis K 2003 *Phys. Rev. Lett.* **90** 241101 (*Preprint* arXiv:astro-ph/0303171)
- Buras R, Rampp M, Janka H-T and Kifonidis K 2006 *Astron. Astrophys.* **447** 1049 (*Preprint* arXiv:astro-ph/0507135)
- Burrows A, Hayes J and Fryxell B A 1995 *Astrophys. J.* **450** 830 (*Preprint* arXiv:astro-ph/9506061)
- Cadonati L, Calaprice F P and Chen M C 2002 *Astropart. Phys.* **16** 361 (*Preprint* arXiv:hep-ph/0012082)
- Cardall C Y 2007 *Preprint* arXiv:astro-ph/0701831
- Chakraborty S, Choubey S, Dasgupta B and Kar K 2008 *JCAP* **0809** 013 (*Preprint* arXiv:0805.3131)
- Chatterjee S *et al* 2005 *Astrophys. J. Lett.* **630** L61 (*Preprint* arXiv:astro-ph/0509031)
- Choubey S, Harries N P and Ross G G 2007 *Phys. Rev. D* **76** 073013 (*Preprint* arXiv:hep-ph/0703092)
- Chugai N N and Utrobin V P 2000 *Astron. Astrophys.* **354** 557 (*Preprint* arXiv:astro-ph/9906190)

- Colgate S A, Grasberger W H and White R H 1961 *Astron. J.* **66** 280
- Colgate S A and Johnson M H 1960 *Phys. Rev. Lett.* **5** 235
- Cordes J M, Romani R W and Lundgren S C 1993 *Nature* **362** 133
- Dasgupta B and Dighe A 2007 *Phys. Rev. D* **75** 093002 (*Preprint* arXiv:hep-ph/0510219)
- Dasgupta B and Dighe A 2008 *Phys. Rev. D* **77** 113002 (*Preprint* arXiv:0712.3798)
- Dasgupta B, Dighe A and Mirizzi A 2008a *Phys. Rev. Lett.* **101** 171801 (*Preprint* arXiv:0802.1481)
- Dasgupta B, Dighe A, Mirizzi A and Raffelt G G 2008b *Phys. Rev. D* **78** 033014 (*Preprint* arXiv:0805.3300)
- Dasgupta B, Dighe A, Mirizzi A and Raffelt G G 2008c *Phys. Rev. D* **77** 113007 (*Preprint* arXiv:0801.1660)
- Davis R, Cleveland B T and Rowley J K 1984 *AIP Conf. Proc.* **123** 1037
- Davis R, Harmer D S and Hoffman K C 1968 *Phys. Rev. Lett.* **20** 1205
- Dessart L, Burrows A, Ott C D, Livne E, Yoon S-C and Langer N 2006 *Astrophys. J.* **644** 1063 (*Preprint* arXiv:astro-ph/0601603)
- Dighe A S and Smirnov A Y 2000 *Phys. Rev. D* **62** 033007 (*Preprint* arXiv:hep-ph/9907423)
- Dornic D *et al* (ANTARES) 2008 *Preprint* arXiv:0810.1416
- Dotani T, Hayashida K, Inoue H, Itoh M and Koyama K 1987 *Nature* **330** 230
- Duan H, Fuller G M and Carlson J 2008a *Comput. Sci. Disc.* **1** 015007 (*Preprint* arXiv:0803.3650)
- Duan H, Fuller G M, Carlson J and Qian Y-Z 2006a *Phys. Rev. Lett.* **97** 241101 (*Preprint* arXiv:astro-ph/0608050)
- Duan H, Fuller G M, Carlson J and Qian Y-Z 2006b *Phys. Rev. D* **74** 105014 (*Preprint* arXiv:astro-ph/0606616)
- Duan H, Fuller G M, Carlson J and Qian Y-Z 2007a *Phys. Rev. D* **75** 125005 (*Preprint* arXiv:astro-ph/0703776)
- Duan H, Fuller G M, Carlson J and Qian Y-Z 2007b *Phys. Rev. Lett.* **99** 241802 (*Preprint* arxiv:0707.0290)
- Duan H, Fuller G M, Carlson J and Qian Y-Z 2008b *Phys. Rev. Lett.* **100** 021101 (*Preprint* arXiv:0710.1271)
- Duan H, Fuller G M and Qian Y-Z 2006c *Phys. Rev. D* **74** 123004 (*Preprint* arXiv:astro-ph/0511275)
- Duan H, Fuller G M and Qian Y-Z 2007c *Phys. Rev. D* **76** 085013 (*Preprint* arxiv:0706.4293)
- Duan H, Fuller G M and Qian Y-Z 2008c *Preprint* arXiv:0808.2046
- Duan H, Fuller G M and Qian Y-Z 2008d *Phys. Rev. D* **77** 085016 (*Preprint* arXiv:0801.1363)
- Duncan R C, Shapiro S L and Wasserman I 1986 *Astrophys. J.* **309** 141
- Erickson E F, Haas M R, Colgan S W J, Lord S D, Burton M G, Wolf J, Hollenbach D J and Werner M 1988 *Astrophys. J. Lett.* **330** L39
- Esteban-Pretel A, Mirizzi A, Pastor S, Tomàs R, Raffelt G G, Serpico P D and Sigl G 2008a *Phys. Rev. D* **78** 085012 (*Preprint* arXiv:0807.0659)
- Esteban-Pretel A, Pastor S, Tomas R, Raffelt G G and Sigl G 2007 *Phys. Rev. D* **76** 125018 (*Preprint* arxiv:0706.2498)
- Esteban-Pretel A, Pastor S, Tomas R, Raffelt G G and Sigl G 2008b *Phys. Rev. D* **77** 065024 (*Preprint* arXiv:0712.1137)
- Fetter J, McLaughlin G C, Balantekin A B and Fuller G M 2003 *Astropart. Phys.* **18** 433 (*Preprint* arXiv:hep-ph/0205029)

- Fogli G, Lisi E, Marrone A and Tamborra I 2008 *Preprint* arXiv:0812.3031
- Fogli G, Lisi E, Mirizzi A and Montanino D 2006a *JCAP* **0606** 012 (*Preprint* arXiv:hep-ph/0603033)
- Fogli G L, Lisi E, Marrone A and Mirizzi A 2007 *JCAP* **0712** 010 (*Preprint* arxiv:0707.1998)
- Fogli G L, Lisi E, Marrone A and Palazzo A 2006b *Prog. Part. Nucl. Phys.* **57** 742
- Fogli G L, Lisi E, Mirizzi A and Montanino D 2003 *Phys. Rev. D* **68** 033005 (*Preprint* arXiv:hep-ph/0304056)
- Friedland A and Gruzinov A 2006 *Preprint* arXiv:astro-ph/0607244
- Friedland A and Lunardini C 2003a *JHEP* **0310** 043 (*Preprint* arXiv:hep-ph/0307140)
- Friedland A and Lunardini C 2003b *Phys. Rev. D* **68** 013007 (*Preprint* arXiv:hep-ph/0304055)
- Fuller G M, Kusenko A and Petraki K 2009 *Phys. Lett. B* **670** 281 (*Preprint* arXiv:0806.4273)
- Fuller G M, Mayle R W, Meyer B S and Wilson J R 1992 *Astrophys. J.* **389** 517
- Fuller G M, Mayle R W, Wilson J R and Schramm D N 1987 *Astrophys. J.* **322** 795
- Fuller G M and Qian Y-Z 2006 *Phys. Rev. D* **73** 023004 (*Preprint* arXiv:astro-ph/0505240)
- Gava J, Kneller J, Volpe C and McLaughlin G C 2009 *Preprint* arXiv:0902.0317
- Gava J and Volpe C 2008 *Phys. Rev. D* **78** 083007 (*Preprint* arXiv:0807.3418)
- Halprin A 1986 *Phys. Rev. D* **34** 3462
- Hannestad S, Raffelt G G, Sigl G and Wong Y Y Y 2006 *Phys. Rev. D* **74** 105010 (*Preprint* arXiv:astro-ph/0608695)
- Hidaka J and Fuller G M 2007 *Phys. Rev. D* **76** 083516 (*Preprint* arXiv:0706.3886)
- Hillebrandt W and Mueller E 1981 *Astron. Astrophys.* **103** 147
- Hirata K *et al* (KAMIOKANDE-II) 1987 *Phys. Rev. Lett.* **58** 1490
- Hix W R, Messer O E B, Mezzacappa A, Liebendörfer M, Sampaio J, Langanke K, Dean D J and Martínez-Pinedo G 2003 *Phys. Rev. Lett.* **91** 201102
- Hughes J P, Rakowski C E, Burrows D N and Slane P O 2000 *Astrophys. J. Lett.* **528** L109 (*Preprint* arXiv:astro-ph/9910474)
- Hwang U *et al* 2004 *Astrophys. J. Lett.* **615** L117 (*Preprint* arXiv:astro-ph/0409760)
- Ikeda M *et al* (Super-Kamiokande) 2007 *Astrophys. J.* **669** 519 (*Preprint* arXiv:0706.2283)
- Iwakami W, Kotake K, Ohnishi N, Yamada S and Sawada K 2008 *Astrophys. J.* **678** 1207 (*Preprint* arXiv:0710.2191)
- Jachowicz N and McLaughlin G C 2006 *Phys. Rev. Lett.* **96** 172301 (*Preprint* arXiv:nucl-th/0604046)
- Jachowicz N, McLaughlin G C and Volpe C 2008 *Phys. Rev. C* **77** 055501 (*Preprint* arXiv:0804.0360)
- Janka H-T and Mueller E 1994 *Astron. Astrophys.* **290** 496
- Janka H-T and Mueller E 1995 *Astrophys. J. Lett.* **448** L109
- Janka H-T and Mueller E 1996 *Astron. Astrophys.* **306** 167
- Kachelrieß M and Tomàs R 2001 *Phys. Rev. D* **64** 073002 (*Preprint* arXiv:hep-ph/0104021)
- Katsuda S, Tsunemi H, Miyata E, Mori K, Namiki M, Nemes N and Miller E D 2008 *Pub. Astron. Soc. Japan* **60** 107 (*Preprint* arXiv:0803.0172)
- Kim C W, Kim J and Sze W K 1988 *Phys. Rev. D* **37** 1072
- Kim C W, Sze W K and Nussinov S 1987 *Phys. Rev. D* **35** 4014
- Kitaura F S, Janka H-T and Hillebrandt W 2006 *Astron. Astrophys.* **450** 345 (*Preprint* arXiv:astro-ph/0512065)

- Kneller J P and McLaughlin G C 2006 *Phys. Rev. D* **73** 056003 (*Preprint* arXiv:hep-ph/0509356)
- Kneller J P and McLaughlin G C 2009 Three flavor neutrino oscillations in matter (in preparation)
- Kneller J P, McLaughlin G C and Brockman J 2008 *Phys. Rev. D* **77** 045023 (*Preprint* arXiv:0705.3835)
- Kostelecký V A and Samuel S 1993 *Phys. Lett. B* **318** 127
- Kostelecký V A and Samuel S 1995 *Phys. Rev. D* **52** 621 (*Preprint* arXiv:hep-ph/9506262)
- Krastev P I and Smirnov A Y 1989 *Phys. Lett. B* **226** 341
- Kuo T K and Pantaleone J 1988 *Phys. Rev. D* **37** 298
- Kuo T K and Pantaleone J 1989a *Phys. Rev. D* **39** 1930
- Kuo T K and Pantaleone J T 1989b *Rev. Mod. Phys.* **61** 937
- Landau L D and Lifshitz E M 1977 *Quantum Mechanics: non-relativistic theory* 3rd ed (Oxford: Pergamon)
- Leonard D C *et al* 2006 *Nature* **440** 505 (*Preprint* arXiv:astro-ph/0603297)
- Li H, McCray R and Sunyaev R A 1993 *Astrophys. J.* **419** 824
- Liebendörfer M, Mezzacappa A, Thielemann F-K, Messer O E, Hix W R and Bruenn S W 2001 *Phys. Rev. D* **63** 103004 (*Preprint* arXiv:astro-ph/0006418)
- Loreti F N and Balantekin A B 1994 *Phys. Rev. D* **50** 4762
- Loreti F N, Qian Y-Z, Fuller G M and Balantekin A B 1995 *Phys. Rev. D* **52** 6664 (*Preprint* arXiv:astro-ph/9508106)
- Lunardini C, Muller B and Janka H-T 2008 *Phys. Rev. D* **78** 023016 (*Preprint* arXiv:0712.3000)
- Lunardini C and Smirnov A Y 2003 *JCAP* **0306** 009 (*Preprint* arXiv:hep-ph/0302033)
- Lyne A G and Lorimer D R 1994 *Nature* **369** 127
- Martínez-Pinedo G 2008 *J. Phys. G* **35** 014057
- Matz S M, Share G H, Leising M D, Chupp E L and Vestrand W T 1988 *Nature* **331** 416
- Mazurek T J 1982 *Astrophys. J. Lett.* **259** L13
- Mezzacappa A 2005 *Annu. Rev. Nucl. Part. Sci.* **55** 467
- Mezzacappa A, Calder A C, Bruenn S W, Blondin J M, Guidry M W, Strayer M R and Umar A S 1998 *Astrophys. J.* **495** 911 (*Preprint* arXiv:astro-ph/9709188)
- Mezzacappa A, Liebendörfer M, Messer O E, Hix W R, Thielemann F-K and Bruenn S W 2001 *Phys. Rev. Lett.* **86** 1935 (*Preprint* arXiv:astro-ph/0005366)
- Mikheyev S P and Smirnov A Y 1985 *Yad. Fiz.* **42** 1441 (*Sov. J. Nucl. Phys.* **42** 913)
- Mikheyev S P and Smirnov A Y 1986 *'86 Massive Neutrinos in Astrophysics and in Particle Physics*, edited by O Frackler and J Trân Thanh Vân (Gif-sur-Yvette: Editions Frontières) p 355
- Nötzold D 1987 *Phys. Lett. B* **196** 315
- Nötzold D and Raffelt G 1988 *Nucl. Phys. B* **307** 924
- Ohnishi N, Iwakami W, Kotake K, Yamada S, Fujioka S and Takabe H 2008 *J. Phys. Conf. Ser.* **112** 042018
- Pantaleone J T 1992 *Phys. Rev. D* **46** 510
- Pastor S and Raffelt G 2002 *Phys. Rev. Lett.* **89** 191101 (*Preprint* arXiv:astro-ph/0207281)
- Pastor S, Raffelt G G and Semikoz D V 2002 *Phys. Rev. D* **65** 053011 (*Preprint* arXiv:hep-ph/0109035)

- Pastorello A *et al* 2007 *Nature* **449** 1 (*Preprint* arXiv:0710.3753)
- Qian Y-Z and Fuller G M 1995a *Phys. Rev. D* **52** 656 (*Preprint* arXiv:astro-ph/9502080)
- Qian Y-Z and Fuller G M 1995b *Phys. Rev. D* **51** 1479 (*Preprint* arXiv:astro-ph/9406073)
- Qian Y-Z, Fuller G M, Mathews G J, Mayle R W, Wilson J R and Woosley S E 1993 *Phys. Rev. Lett.* **71** 1965
- Raffelt G G 2008 *Phys. Rev. D* **78** 125015 (*Preprint* arXiv:0810.1407)
- Raffelt G G and Sigl G G R 2007 *Phys. Rev. D* **75** 083002 (*Preprint* arXiv:hep-ph/0701182)
- Raffelt G G and Smirnov A Y 2007a *Phys. Rev. D* **76** 125008 (*Preprint* arxiv:0709.4641)
- Raffelt G G and Smirnov A Y 2007b *Phys. Rev. D* **76** 081301(R) (*Preprint* arxiv:0705.1830)
- Rampp M and Janka H-T 2000 *Astrophys. J. Lett.* **539** L33 (*Preprint* arXiv:astro-ph/0005438)
- Samuel S 1993 *Phys. Rev. D* **48** 1462
- Sawyer R F 1990 *Phys. Rev. D* **42** 3908
- Sawyer R F 1994 *Phys. Rev. D* **50** 1167
- Sawyer R F 2008 *Preprint* arXiv:0803.4319
- Scarborough J B 1958 *The Gyroscope, Theory and Application* (New York: Interscience)
- Schafer A and Koonin S E 1987 *Phys. Lett. B* **185** 417
- Scheck L, Kifonidis K, Janka H-T and Müller E 2006 *Astron. Astrophys.* **457** 963 (*Preprint* arXiv:astro-ph/0601302)
- Schirato R C and Fuller G M 2002 *Preprint* arXiv:astro-ph/0205390
- Sedov L I 1959 *Similarity and Dimensional Methods in Mechanics* (New York: Academic Press)
- Sharp M K, Beacom J F and Formaggio J A 2002 *Phys. Rev. D* **66** 013012 (*Preprint* arXiv:hep-ph/0205035)
- Sigl G and Raffelt G 1993 *Nucl. Phys. B* **406** 423
- Strack P and Burrows A 2005 *Phys. Rev. D* **71** 093004 (*Preprint* arXiv:hep-ph/0504035)
- Strumia A and Vissani F 2006 *Preprint* arXiv:hep-ph/0606054
- Stückelberg, E C G 1932 *Helv. Phys. Acta.* **5** 369
- Sunyaev R *et al* 1987 *Nature* **330** 227
- Takahashi K, Sato K, Dalhed H E and Wilson J R 2003 *Astropart. Phys.* **20** 189 (*Preprint* arXiv:astro-ph/0212195)
- Taylor J H, Manchester R N and Lyne A G 1993 *Astrophys. J. Suppl. Ser.* **88** 529
- Thompson T A, Burrows A and Pinto P A 2003 *Astrophys. J.* **592** 434 (*Preprint* arXiv:astro-ph/0211194)
- Tomàs R, Kachelrieß M, Raffelt G, Dighe A, Janka H-T and Scheck L 2004 *JCAP* **0409** 015 (*Preprint* arXiv:astro-ph/0407132)
- van Riper K A 1982 *Astrophys. J.* **257** 793
- Voloshin M B, Vysotsky M I and Okun L B 1986 *Zh. Eksp. Teor. Fiz.* **91** 754 (*Sov. Phys. JETP* **64** 446)
- Wang L, Howell D A, Höflich P and Wheeler J C 2001 *Astrophys. J.* **550** 1030
- Weaver T A, Zimmerman G B and Woosley S E 1978 *Astrophys. J.* **225** 1021
- Winkler P F and Petre R 2007 *Astrophys. J.* **670** 635 (*Preprint* arXiv:astro-ph/0608205)
- Wolfenstein L 1978 *Phys. Rev. D* **17** 2369
- Woosley S E, Heger A and Weaver T A 2002 *Rev. Mod. Phys.* **74** 1015
- Zener C 1932 *Proc. R. Soc. A* **137** 696